Graduate School of the Social and Behavioural Sciences

Universität Konstanz

GSBS Working Paper No. 2022-01

Identifying Proxy VARs with Restrictions on the Forecast Error Variance

Tilmann Härtl

December 2022

Graduate School of the Social and Behavioural Sciences

The Graduate School of the Social and Behavioural Sciences (GSBS) at the University of Konstanz is an interdisciplinary doctoral school, which aims to provide a state-of-the art training and research environment for doctoral candidates.

Our doctoral candidates have backgrounds in Biology, Economics, Linguistics, Political Science and Public Administration, Physics, Psychology, Sociology, Statistics. In addition, the GSBS offers specialisations in Collective Behaviour, Decision Sciences, and Inequality. The renowned international faculty of the GSBS conducts cutting edge research. Academic excellence permeates both our research agenda and training measures.

GSBS – Graduate School of the Social and Behavioural Sciences

University of Konstanz
Box 146
78457 Konstanz

Phone: +49 (0)7531 88 3633
Fax: +49 (0)7531 88 5193
E-mail: gsbs.office@uni-konstanz.de

-gsdbs.uni-konstanz.de

ISSN: 2365-4120
December 2022

© 2022 by the author(s)

Identifying Proxy VARs with Restrictions on the Forecast Error Variance*

Tilmann Härtl

Department of Economics, University of Konstanz

tilmann.haertl@uni-konstanz.de

December 1, 2022

Abstract

The proxy VAR framework requires additional restrictions to disentangle the structural shocks when multiple shocks are identified using multiple instruments. I propose to employ restrictions on the forecast error variance (FEV). Less restrictive assumptions that bound the contributions to the FEV can replace or accompany inequality restrictions on e.g. the impulse responses. This enables to sharpen the set identification of the structural parameters. Furthermore, assuming one shock maximizes the contribution to the FEV of a target variable (Max-Share) can be used to point identify the structural parameters. I show under which circumstances this strategy succeeds and propose an augmentation to the Max-Share framework in cases it is prone to bias concerns. Point identification is achieved without the need for strict equality restrictions, but limited to the case of two proxies which identify two shocks.

*Financial support by the German Science Foundation (DFG) grant number BR 2941/3-2 is gratefully acknowledged. Further, I thank the seminar participants of the IAAE and ESEM conferences for helpful comments and remarks.

1 Introduction

External instruments, also called proxies, are a powerful tool for the identification of structural vector autoregressions (SVARs). Since the proxy VAR framework was introduced by Stock and Watson (2012) and Mertens and Ravn (2013) they are highly prevalent in the SVAR literature, e.g. Gertler and Karadi (2015), Piffer and Podstawski (2018) or Lakdawala (2019). The proxies contain external information regarding the shocks that one wants to identify. Reminiscent to the classical instrumental variables framework the proxies need to satisfy two conditions. They have to be related to the target shocks of interest (relevancy) while being unrelated to the remaining structural shocks that are not identified (exogeneity). However, if multiple shocks are identified with multiple instruments, Mertens and Ravn (2013) show that the information of the proxies alone is not sufficient to disentangle the structural shocks and additional identifying restrictions are needed.

Obvious candidates for these additional restriction are e.g. restrictions on the structural impulse response functions (IRFs) like strict equality restrictions or less strict sign restrictions. This paper focuses on the identification via the forecast error variance (FEV) decomposition. The key merit of restrictions on the FEV decomposition is that they do not impose restrictions on the structural impulse response functions which are often the key element of interest in the structural VARs. In a perfect scenario, they have the potential to identify the structural IRFs without the need to impose any structure on these response parameters. Yet, the FEV restrictions can also be used in conjunction with restrictions on the impulse responses in particular and with other restrictions in general. Either to weaken the requirements on the other restrictions or to simply sharpen the identification of existing identification schemes. This paper discusses two different approaches that use restrictions on the FEV for identification.

Firstly, bounds on the contribution of the target shocks to the FEV of specified variables can be used as identifying restrictions. These bounds were introduced by Volpicella (2022) and this paper describes how to use them in the proxy VAR framework. The bounds serve as inequality restrictions and, similar to other identification schemes that rely on inequality restrictions (e.g. sign restrictions), the structural parameters are set identified. Hence, the bound restrictions are subject to the trade-off between less strict assumptions and less sharp identification which is common to set identification schemes. The narrower one sets the bound constraints the sharper the identification. Yet narrower bounds represent more strict assumptions on the underlying process.

The bound restrictions are useful in two different ways. On their own, they can identify the structural IRFs without the need to impose any restrictions on them. Yet, in combination with other restrictions they help to sharpen the set identification. Suppose, for example, the structural shocks are identified with rather weak sign restrictions. Instead of imposing more strict sign restrictions on impulse responses, adding bound restrictions on the FEV can help to sharpen the identification. Building on the work of Volpicella (2022) this paper describes how these bound restrictions can be used in the proxy VAR and building on Giacomini, Kitagawa, and Read (2022) it provides robust Bayesian inference for the structural parameters of interest.

Second, one can also achieve sharp point identification via restrictions on the FEV. In doing so, the key assumption is that one shock maximizes the contribution to the FEV of a specific variable, i.e. a technology shock is identified as the shock with maximum contribution to the FEV of a TFP measurement (Francis, Owyang, Roush, & DiCecio, 2014). This strategy dates back to Faust (1998) and Uhlig (2004a) and was originally an alternative to the bias prone long-run restrictions. Francis et al. (2014) coined the term 'Max-Share' for this identification strategy and in the following I use this expression to refer to it. In the literature it has, for instance, been used by Barsky and Sims (2011) to identify technology news shocks and by Ben Zeev and Pappa (2017) to identify defence spending news shocks.

The Max-Share portion of this paper only discusses the case of two shocks being identified with two proxies. In practice most of the applications with multiple proxies are limited to the use of two instruments, e.g. Mertens and Ravn (2013), Piffer and Podstawski (2018) or Lakdawala (2019). Hence, the two instrument case is highly relevant for empirical work and it has the nice advantage that the identification of one shock with the Max-Share approach also yields identification of the second shock at the same time. The key merit of fusing proxy VARs and the Max-Share approach is that sharp point identification of the structural parameters is achieved without the need for strict equality restrictions.

Yet, Dieppe, Neville, and Kindberg-Hanlon (2019) point out that the Max-Share framework has a problem with confounding shocks leading to bias in the structural parameters. Shocks, other than the target shock of the Max-Share approach, are confounders if they also contribute to the FEV of the target variable. The proxy VAR partially solves this concern as shocks that are not related to the proxies are ruled out as confounders. I show that if one the two shocks related to the proxies exclusively contributes to the FEV of the target variable, the Max-Share approach correctly identifies the true structural parameters. Other potential confounding shocks, not related to the proxies, do not bias the results.

However, in practice this exclusive contribution is not always a suitable assumption and in this case I propose to augment the Max-Share framework with an inequality constraint to eliminate the Max-Share bias. I provide sufficient conditions for the inequality constraint under which the augmented Max-Share approach successfully identifies the structural parameters. One condition simply depends on the functional form of the quantity that is constrained, i.e. an impulse response. This condition can be checked easily in practice. A second condition though, requires the economic intuition behind the inequality constraint to be correct. In order to assess the plausibility of this condition one needs to provide convincing evidence or reasoning for the imposed constraint. Similar to other identifying restrictions this reasoning can be based on economic theory, previous results or simply economic intuition.

Two different types of inequality constraints serve as an example. Firstly, a constraint on a single impulse response at a single horizon can be sufficient to remove the Max-Share bias and I show how to assess whether the imposed constraint is suitable or not. Second, I describe under which circumstances a constraint on the difference in impulse responses of the two identified shock on a single variable, and again at a single horizon, helps to identify the underlying structural parameters. A simulation study illustrates the theoretical results and shows how to assess the sufficient conditions in a potential empirical application. Further, I show under which circumstances the Max-Share bias is guaranteed to decrease in the presence of an inequality constraint. The simulation study also illustrates this. Lastly, I describe how to conduct inference for the structural parameters in the proxy Max-Share framework.

In summary, I present two different ways one can make use of restrictions on the FEV decomposition. On the one hand, one can employ the less restrictive approach via bounds on the FEV, which can also be easily used in combination with other set identifying restrictions in order to improve upon existing set identification schemes. On the other hand, the Max-Share framework which sharply point identifies the structural model but requires stronger assumptions and and a good economic intuition for a potential inequality constraint. Hence, depending on the prior knowledge about the structure in the FEV a suitable identification scheme can be chosen.

Section 2 commences with the introduction of the baseline SVAR framework and the proxy VAR. Section 3 describes the usage of restrictions on the FEV for the identification of the structural VAR. It starts with the more general set identification approach via the bounds on the FEV and ends with the more strict point identification via the Max-Share framework. Section 4 presents the results of the simulation study.

2 Econometric Framework

2.1 The Structural VAR

The starting point is the k-dimensional stationary structural VAR(p) model:

$$y_t = \sum_{m=1}^{p} A_m y_{t-l} + B w_t, \quad t = 1, ...T, \tag{1}$$

where the $k \times 1$ vector w_t depicts the economically meaningful structural shocks (e.g. Kilian & Lütkepohl, 2017). The $k \times k$ impact matrix B maps the the structural shocks into the reduced form innovations, $u_t = Bw_t$. The elements of the $k \times 1$ white noise vector u_t are the reduced form innovations. To shorten the notation one can rewrite the SVAR in (1) as:

$$y_t = A x_t + B w_t, \quad t = 1, ...T, \tag{2}$$

with $x_t = (y'_{t-1}, ..., y'_{t-p})'$ and $A = (A_1, ..., A_p)$. A constant is omitted for the brevity of the notation but it can be included in a straightforward way.

Common to most identification strategies is the normalization $\mathbb{E}(w_t w_t') \equiv \Sigma_w = I_K$, which yields the set of covariance restriction $\mathbb{E}(u_t u_t') \equiv \Sigma = BB'$. Without further assumptions these restrictions do not suffice to pin down the structural parameters as the resulting system of equations has many possible solutions. The Cholesky decomposition of Σ, denoted by Σ_c, satisfies these covariance restrictions. Yet, they will also hold for every rotation with an $k \times k$ orthonormal matrix Q, $\Sigma = \Sigma_c \Sigma_c' = \Sigma_c Q Q' \Sigma_c'$. Giacomini et al. (2022) refer to this representation of the SVAR as the 'orthogonal reduced form'.

Under stability of the VAR polynomial the moving average representation of the SVAR is given by:

$$y_t = \sum_{m=0}^{\infty} C_m \Sigma_c Q w_{t-m}, \quad t = 1, ...T, \tag{3}$$

where the $k \times k$ matrices C_m contain the moving average coefficients which give the response of the system to the reduced form innovations m periods ago. The impulse response of variable i to shock j at horizon h is given by:

$$\eta_{i,j,h} = e_i' C_h \Sigma_c q_j, \tag{4}$$

where e_i is the ith column of I_k and q_j is the jth column of Q.

Apart from the impulse response functions the FEV decomposition is are an element of interest in the SVARs. In this paper the FEV decomposition is particularly of importance as identifying restrictions are placed on it. To formalize the FEV decomposition let the h-step-ahead forecast of y_t be:

$$y_{t+h|t} = \sum_{m=0}^{\infty} C_{h+m} u_{t-m}. \tag{5}$$

The h-step ahead forecast error is then given by:

$$y_{t+h} - y_{t+h|t} = \sum_{m=0}^{h-1} C_m \Sigma_c Q w_{t+h-m}, \tag{6}$$

and the h-step ahead forecast error covariance matrix is represented by:

$$\Omega(h) = \sum_{m=0}^{h-1} C_m \Sigma_c Q Q' \Sigma_c' C_m' = \sum_{m=0}^{h-1} C_m \Sigma C_m'. \tag{7}$$

The contribution from shock j to the total forecast variance of variable i at horizon h is then:

$$\Omega_{i,j}(h) = \frac{e_i'(\sum_{m=0}^{h-1} C_m \Sigma_c q_j q_j' \Sigma_c' C_m')e_i}{e_i'(\sum_{m=0}^{h-1} C_m \Sigma C_m')e_i}. \tag{8}$$

In order to identify the structural parameters of interest restrictions have to be placed on the model. As mentioned before two different identification schemes exist. Set identification amounts to finding all the rotation matrices Q that satisfy the identification restrictions. In turn, they define the identified set for e.g. the impulse response functions or the FEV decomposition. Common set identification restrictions are, for instance, inequality restrictions on the structural impulse responses. The stricter the identifying restrictions, the smaller the identified set. In point identification schemes the restrictions are such that only one admissible rotation matrix Q exists. The typical point identification restrictions are equality restrictions on the elements of the impact matrix B. For example, $k(k-1)/2$ independent equality restrictions on B are sufficient to point identify the structural parameters.

The proxy VAR framework that is introduced in the next subsection allows for both, point and set identification. If one shock is identified using one proxy variable the parameters are point identified up to sign and scale. With multiple shocks and multiple proxies additional restrictions are needed in order to disentangle the shocks. In the latter case the just mentioned sign or equality restrictions are one possibility and depending on the type of imposed restrictions the structural parameters are either point or set identified.

2.2 Proxy VAR

For the proxy VAR framework I loosely follow the very general framework by Giacomini et al. (2022) as the inference for the set identification part will be based on their work. As in the standard instrumental variable (IV) framework, the proxy variables - also called instruments interchangeably - have to satisfy two key assumptions. Without loss of generality, let z_t be a $l \times 1$ vector of instruments that are related to the first l structural shocks in w_t. The two following two conditions have to be satisfied:

$$\mathbb{E}(z_t w_{(1:l),t}) = \Psi \quad \text{and} \quad \mathbb{E}(z_t w_{(l+1:k),t}) = 0, \tag{9}$$

where Ψ is an $l \times l$ matrix of full rank. These two conditions resemble the relevance and exogeneity conditions of the standard IV approach. The instruments have to be related to the target shocks and unrelated to the remaining structural shocks. Assume that the proxies follow:

$$\Gamma_0 z_t = \Lambda w_t + \sum_{m=1}^{p_z} \Gamma_m z_{t-m} + \nu_t, \quad t = 1, ..., T. \tag{10}$$

The process in (10) indicates that the proxies are related to the structural shocks. Giacomini et al. (2022) assume that $(w_t', \nu_t')'|\mathcal{F}_{t-1} \sim N(0_{(k+l)\times 1}, I_{k+l})$, where $\mathcal{F}_{t-1}$ is the information set at time $t-1$.

The assumptions in (9) together with process (10) yield:

$$\mathbb{E}(z_t w_t') = \Gamma_0^{-1}\Lambda = [\Psi, 0_{l\times(k-l)}]. \tag{11}$$

Plugging model (2) into the process in (10) and left-multiplying by Γ_0^{-1} yields:

$$z_t = D y_t + G x_t + \sum_{m=1}^{p_z} H_m z_{t-m} + \upsilon_t, \quad t = 1, ..., T, \tag{12}$$

where $D = \Gamma_0^{-1}\Lambda B^{-1}, G = -\Gamma_0^{-1}\Lambda A$ and $H_m = \Gamma_0^{-1}\Gamma_l$ for each $m = 1, ..., p_z$.

Giacomini et al. (2022) show that (11) can also be represented by:

$$\mathbb{E}(z_t w_t') = D\Sigma_c Q = [\Psi, 0_{l\times(k-l)}], \tag{13}$$

implying that the relevance assumption rank$(\Psi) = l$ is fulfilled if and only if rank$(D) = l$. The exogeneity and relevance assumption regarding the proxies restricts the rotation matrices Q such that they follow the structure in (13). In this fashion the proxy VAR shrinks the identified set.

In the following I deviate from the notation of Giacomini et al. (2022) and use the proxy VAR framework by Piffer and Podstawski (2018). This allows me to handle both the bounds on the FEVD and the combination with Max-Share approach in the same proxy VAR framework. The next section describes how the robust Bayesian inference algorithm of Giacomini et al. (2022) is adapted to the representation of the proxy SVAR below.

Following Piffer and Podstawski (2018), I decompose the reduced form errors into two components:

$$u_t = B_z w_{(1:l),t} + B_{-z} w_{(l+1:k),t}, \quad t = 1, ..., T, \tag{14}$$

where B_z is the $k \times l$ block of the impact matrix B that contains the first l colums and B_{-z} is the according remaining part of B. B_z contains the structural parameters of the shocks related to the proxies whose identification is the goal of the proxy VAR. I refer to this matrix as the 'proxy impact matrix'. Considering (14) together with the assumption regarding the proxies in (9) yields $\mathbb{E}(u_t z_t') = B_z \Psi' = Z$. Equation (13) lets me rewrite this expected value:

$$\mathbb{E}(u_t z_t') = B\mathbb{E}(w_t z_t') = B\mathbb{E}(z_t w_t')' = \Sigma D', \tag{15}$$

with $B = \Sigma_c Q$ and $\mathbb{E}(z_t w_t') = D\Sigma_c Q$. Hence, $\Sigma D' = Z = B_z \Psi'$. Partitioning the matrix $\Sigma D'$ and B_z yields:

$$\Sigma D' = Z = \begin{pmatrix} Z_1 \\ Z_2 \end{pmatrix} \text{ and } B_z = \begin{pmatrix} B_{11} \\ B_{21} \end{pmatrix} \tag{16}$$

and thus

$$B_{21} = Z_2 Z_1^{-1} B_{11} = Z_l B_{11}, \tag{17}$$

where Z_1 is the upper $l \times l$ block of the matrix Z and B_{11} is the upper $l \times l$ block of B_z. Hence,

$$B_z = \begin{pmatrix} B_{11} \\ Z_l B_{11} \end{pmatrix}, \tag{18}$$

and if the upper $l \times l$ block B_{11} is identified the remaining block of the proxy impact matrix is identified as well. In order to identify the upper block of B_z partition the matrices of the standard covariance restrictions $\mathbb{E}(u_t u_t') \equiv \Sigma = BB'$ such that:

$$\begin{pmatrix} \Sigma_{11} & \Sigma_{12} \\ \Sigma_{21} & \Sigma_{22} \end{pmatrix} = \begin{pmatrix} B_{11} & B_{12} \\ B_{21} & B_{22} \end{pmatrix} \begin{pmatrix} B_{11} & B_{21} \\ B_{12} & B_{22} \end{pmatrix}, \tag{19}$$

where Σ_{11} is the upper left $l \times l$ block of Σ. B_{11} is again the upper $l \times l$ block of B_z and therefore the upper left block of B. The remaining blocks of the two matrices have the according dimensions. It can be shown that $B_{11}B_{11}' = \Sigma_{11} - B_{12}B_{12}'$ (see Mertens & Ravn, 2013) with:

$$B_{12}B_{12}' = (\Sigma_{21} - Z\Sigma_{11})'\Pi^{-1}(\Sigma_{21} - Z\Sigma_{11}), \tag{20}$$

$$\Pi = \Sigma_{22} + Z'\Sigma_{11}Z' - \Sigma_{21}Z' - Z\Sigma_{21}'. \tag{21}$$

Similar to the covariance restrictions $\mathbb{E}(u_t u_t') \equiv \Sigma = BB'$, the equation $B_{11} = \Sigma_{11} - B_{12}B_{12}'$ does not pin down the parameters of B_{11} uniquely. Let B_{11}^c be the Cholesky decomposition of $\Sigma_{11} - B_{12}B_{12}'$, then every rotation of B_{11}^c with an $l \times l$ orthonormal matrix Q will also satisfy $B_{11} = B_{11}^c B_{11}^{c'} = B_{11}^c QQ' B_{11}^{c'} = \Sigma_{11} - B_{12}B_{12}'$.

The exogeneity and relevance restriction regarding the proxies is satisfied for B_z by construction. Hence, the identification boils down to finding the set of $l \times l$ orthonormal matrices Q that satisfy the additional identifying restrictions, e.g. inequality restriction on structural parameters. In the next section I describe how inequality restrictions on the FEV like in Volpicella (2022) fit into this framework.

It is also possible to point identify the structural parameters, what again comes down to finding the one rotation matrix for which the restrictions are satisfied. If the resulting recursive structure of B_{11}^c for the contemporaneous impacts of the identified shocks is economically justifiable, the Cholesky decomposition immediately point identifies the structural shocks. This is, for instance, the identification assumption used in Mertens and Ravn (2013) and the corresponding rotation matrix is just $Q = I_l$.

3 Proxy VAR with Restrictions on the FEV

3.1 Proxy VARs with Bounds on the FEV

The bounds on the contributions to the FEV where introduced by Volpicella (2022) and this section applies them to the proxy SVAR framework. In doing so, I loosely follow the notation of Volpicella (2022). Such bounds on the FEV are inequality restrictions in the spirit of the well-known sign restrictions on impulse response parameter, and thus the structural parameters are set identified. Naturally, the challenges the set identification literature deals with also apply to this identification scheme.

3.1.1 Bounding the contribution to the FEV

In the proxy VAR framework the contribution of shock j to the FEV of variable i at horizon h is:

$$\Omega^z_{ij}(h) = \frac{e_i'(\sum_{m=0}^{h-1} C_m B_z q_j q_j' B_z' C_m')e_i}{e_i'(\sum_{m=0}^{h-1} C_m \Sigma C_m')e_i}. \tag{22}$$

Uhlig (2004b) shows that equation (22) can also be written as:

$$\Omega_{i,j}(h) = q_j' R_{i,h} q_j, \tag{23}$$

where

$$R_{i,h} = \frac{\sum_{m=0}^{h-1} c_{i,m}' c_{i,m}}{e_i'(\sum_{m=0}^{h-1} C_m \Sigma C_m')e_i}, \tag{24}$$

with $c_{i,m} = e_i C_m B_z$ is the ith row vector of $C_m B_z$. $R_{i,h}$ is a positive semidefinite and symmetric $l \times l$ real matrix.

Given equation (23) the bounds on the contribution to the FEV of variable i by shock j at horizon h can be represented by:

$$\underline{\tau}_{i,j,h} \leq q_j' R_{i,h} q_j \leq \overline{\tau}_{i,j,h},$$

where $\underline{\tau}_{i,j,h}$ and $\overline{\tau}_{i,j,h}$ depict the lower and upper bound, respectively, and $0 \leq \underline{\tau}_{i,j,h} \leq \overline{\tau}_{i,j,h} \leq 1$. Following the notation of Volpicella (2022), let $\mathcal{I}_j$ be a set of indices that denote whether the FEV of variable i is bounded and $\mathcal{H}_{ij}$ collects the horizons $h = 0, 1, ...$ for which these bounds are imposed. The whole set of bound constraints is then characterized by

$$\underline{\tau}_{i,j,h} \leq q_j' R_{i,h} q_j \leq \overline{\tau}_{i,j,h}, \text{ for } i \in \mathcal{I}_j \text{ and } h \in \mathcal{H}_{ij}.$$

These bounds on the contributions to the FEV can also be applied together with already existing set identifying inequality restrictions, like e.g. sign restrictions. Furthermore, restrictions on the correlations of the proxies with the identified shocks are possible. These type of restrictions constrain the elements of Ψ. They can be checked employing the routine used by Piffer and Podstawski (2018). The identified set is then characterized by all the rotation matrices Q for which these FEV bounds and other potential restrictions are satisfied. As pointed out by Volpicella (2022) such bounds on the FEV contributions can be derived either through economic theory or simply by strong beliefs due to economic intuition.

3.1.2 Nonemptiness of the Set

The bound restrictions, together with potential additional restrictions, are subject to set-identification specific considerations. On the one hand, if the bounds are not restrictive enough one gets potentially large identified sets which yield a fuzzy identification of the underlying structural effects. If, on the other hand, the bounds are too restrictive the identified set might be empty because no structural representation of the model satisfies them.

Unfortunately, no formal guidance helps to assess the restrictions in this regard, what in turn highlights the importance of the economic theory or intuition behind them. Yet, if the identified set is empty, this might be a sign that the imposed restrictions are not reasonable.

Furthermore, it is important to know whether the set is empty for the estimation procedure. Volpicella (2022) provides sufficient conditions for the nonemptiness of the identified set when only one shock is restricted. These sufficient conditions also apply in the same fashion to the proxy VAR framework. Recall that the contribution of the target shock j to the FEV of variable i is:

$$\Omega_{ij}(h) = q_j' R_{i,h} q_j, \tag{25}$$

Let λ_m^{ih} the real eigenvalues of $R_{i,j}$ with $i \in \mathcal{I}_j$, $h \in \mathcal{H}_{ij}$ and $m = 1, ..., l$. Uhlig (2004b) shows that finding the maximum (minimum) of (25) with respect to q_j amounts to finding the largest (smallest) eigenvalue λ_m^{ih} of $R_{i,h}$ and the maximum (minimum) is achieved by using the corresponding eigenvector q_m as a rotation vector q_j. Hence, the eigenvalues λ_m^{ih} correspond to the contributions to the FEV of variable i at horizon h.

Proposition 3.1 adapts Proposition 3.1 of Volpicella (2022) to the proxy VAR framework and gives sufficient conditions for the nonemptiness of the identified set when a single target shock j is restricted. The proof is relegated to the Appendix A.

Proposition 3.1. (Nonemptiness) If the following conditions hold:

(a) $\exists i \in \mathcal{I}_j, \exists h \in \mathcal{H}_{ij} \mid \underline{\tau}_{i,j,h} \leq \lambda_m^{ih} \leq \overline{\tau}_{i,j,h},\ R_{i,h} q_m = \lambda_m^{ih} q_m$ for some $m = 1, ..., l$,

(b) given q_m from (a), $\underline{\tau}_{i,j,h} \leq q_m' R_{i,h} q_m \leq \overline{\tau}_{i,j,h} \forall i \in \mathcal{I}_j$ and $\forall h \in \mathcal{H}_{ij}$, and all other additional restrictions are satisfied,

then the identified set is non-empty and bounded.

The sufficient condition requires to find an eigenvalue λ_m^{ih} which lies inside the imposed bounds on $\Omega_{ij}(h)$. If for $q_j = q_m$ all other identifying restrictions are satisfied the identified set is non-empty.

A difference to Volpicella (2022) is the number of eigenvalues that are available for assessment of the nonemptiness. In the proxy VAR only l eigenvalues are at hand compared to the k eigenvalues in Volpicella (2022). In practice the sufficient conditions will be met more frequently compared to the case with only l eigenvalues. On top of that, the largest and smallest eigenvalue in the proxy VAR case represents the maximum and minimum contribution to the FEV at the specific horizon. Hence, if $l = 2$ only the maximum and minimum contribution can be used to check the nonemptiness. If the bounds do not encompass the extreme values the sufficient conditions are not satisfied. Yet, in practice it might be interesting to set the bounds on the FEVD such that they are close to the maximum or minimum.

Looking at the eigenvalues, one can also quickly see whether the identified set is empty or not. If the upper bound $\overline{\tau}_{i,j,h}$ is smaller than the minimum eigenvalue of $R_{i,h}$ for one of the imposed bounds, or if the lower bound $\underline{\tau}_{i,j,h}$ is larger than the maximum eigenvalue.

If the sufficient conditions of Proposition 3.1 are not fulfilled and the identified set is not found to be empty as described in the previous paragraph, a different approach helps to approximate the nonemptiness of the identified set. As often done in the literature, one can draw a specified number of matrices Q from the orthonormal space. If none of this draws satisfies the restrictions one can conclude that the set is empty.

Lastly, a special case arises when the number of instruments is $l = 2$. Then Proposition 3.1 also helps to detect nonemptiness when both shocks are subject to identification restrictions. Knowing q_m amounts to knowing the whole 2×2 rotation matrix Q_m due to the properties of orthonormal matrices. Hence, in step (b) of Proposition 3.1 also the restrictions on the second shock can be checked.

3.1.3 Estimation and Inference

This subsection introduces the robust Bayesian inference framework by Giacomini et al. (2022). The benefit of this approach is that it avoids specifying a prior over the rotation matrices Q that is not updated by the data. Baumeister and Hamilton (2015) show that when the prior for the rotation matrices Q is a uniform distribution over that space of orthonormal matrices, the common approach in the literature, the structural parameters are influenced by the prior distribution even asymptotically.

The remedy is to use a distribution-free approach. In the robust Bayesian inference the endpoints of the identified set are calculated numerically or analytically if possible. The endpoints, or boundaries, of the identified set are the maximum and minimum values of the structural parameters of interest given all admissible rotation matrices Q. Giacomini et al. (2022) show that this procedure yields prior robust inference over the structural parameters.

As mentioned previously, I adapt the algorithm used in Giacomini et al. (2022) to the specification of the proxy VAR framework in the previous section. I incorporate the exogeneity and relevance restriction regarding the proxies via the proxy impact matrix B_z and only rotate the upper block B_{11} with an orthonormal matrix Q. Apart from the benefit that I can fit bounding the FEVD and the Max-Share approach in the same proxy VAR framework, two additional advantages arise. One merit is that I do not need to draw the rotation matrices Q subject to the exogeneity restriction as depicted in (13). For large iteration counts of the inference algorithm this potentially saves some computation time. Further, I avoid a specific ordering of the variables in the VAR. The ordering convention defined in Giacomini et al. (2022) might be difficult to incorporate in practice when it is not obvious which structural shock is linked to which variable in the VAR system.

To describe the Bayesian algorithm let $\phi \in \Phi$ collect all the reduced form parameters in (2) and (12). For the following algorithm it is not important which prior for ϕ is used as long as one is capable to draw from the posterior distribution of the reduced form parameters. For the results derived in the next sections I follow Giacomini et al. (2022) and use an (improper) Jeffrey's prior.

Suppose that the impulse responses $\eta_{i,j,h} = e_i' C_m B_z q_j$ are the structural parameters of interest. The upper and lower boundary of the identified set with respect to the imposed restrictions are depicted by $u_{i,h}(\phi)$ and $l_{i,h}(\phi)$. Algorithm 1 describes how to conduct robust Bayesian inference for the identified set of $\eta_{i,j,h}$.

Algorithm 1.

Step 1: Obtain draws ϕ from its posterior distribution and compute B_{11}^c.

Step 2: Check whether the identified set is empty. If the set is empty go back to Step 1. If the set is non-empty proceed with Step 3.

Step 3: Compute the boundaries of the identified set:

$$
\begin{aligned}
l_{i,h}(\phi) = & \min_{Q} e_i' C_m B_z q_j \\
s.t \quad & \underline{\tau}_{i,j,h} \leq q_j' R_{i,h}(\phi) q_j \leq \overline{\tau}_{i,j,h}, \quad \forall i \in \mathcal{I}_j \text{ and } \forall h \in \mathcal{H}_{ij}, \\
& QQ' = I_l, \\
& \text{potential sign restrictions and/or restrictions on } \Psi.
\end{aligned}
$$

The upper boundary $u_{i,h}(\phi)$ is obtained analogously.

Step 4: Repeat Steps 2 and 3 N times.

Step 5: Approximate the set of posterior means and the robust credible region as described in Giacomini et al. (2022).

Especially, Step 2 differs from the algorithm of Giacomini et al. (2022) as Proposition 3.1 helps to gauge whether the identified set is empty. If the sufficient conditions of Proposition 3.1 are not fulfilled a specified number of rotation matrices Q are drawn to approximate the set as being empty if none of the draws satisfies the identification restrictions. In this case, Step 2 differs from Giacomini et al. (2022) as the $l \times l$ rotation matrices Q do not need to be drawn considering the exogeneity conditions for the proxies. These conditions are already incorporated in the construction of B_z. Step 3 differs in the specification of the proxy VAR, and thus the dimension of the rotation matrix Q. Second, the added constraint in the maximization problem that represents the restrictions on the FEV are a distinction to the algorithm in Giacomini et al. (2022).

Step 3 poses a nonconvex optimization problem. Hence, the typical approaches to handle with gradient based optimization techniques are necessary. The simple remedy is to use different initial values and to compute the maximum or minimum over the set of solutions which are derived with the different initial values. Giacomini et al. (2022) also provide an algorithm to approximate the boundaries of the identified set in order to check the convergence of the numerical optimization or simply as an alternative.

Algorithm 2. Replace Step 3 of Algortihm 1 with:

Step 3: Draw Q until N draws which satisfy the identification restrictions are reached. For each $Q_n,\ n = 1, ..., N$ compute $\eta_{n,i,j,h} = e_i' C_m B_z q_{n,j}$ and approximate $u_{i,h}(\phi)$ and $l_{i,h}(\phi)$ by the maximum and minimum of $\eta_{n,i,j,h}$ over all N draws.

Montiel Olea and Nesbit (2021) show that the random sampling approximation of Algorithm 2 can be represented as a supervised learning problem. They provide the number of admissible draws of Q that are needed to learn the set with a certain precision. Generally, the approximated set will be smaller than the true set, yet with a sufficient number of draws the approximation error will be small. The theoretical results of Montiel Olea and Nesbit (2021) can be used to judge the precision of the approximation at a certain amount of draws N.

Giacomini et al. (2022) argue that this approximation might be favourable under certain circumstances. Firstly, if the VAR system is large and one is interested in the impulse responses for many variables at many horizons. Drawing many rotation matrices Q is computationally less costly than optimizing for every variable at every horizon. This is especially true with the representation of the proxy VAR used in this paper as it is quite easy to draw simple $l \times l$ rotation matrices considering that l is small in most empirical applications. Second, if not only the impulse responses but also e.g. the FEV decomposition is of interest the approximation has an advantage. Each draw of Q can be used to compute the impulse responses and FEV decomposition of each variable at every horizon, while the optimization has to be carried out for each parameter, variable and horizon individually.

3.2 Proxy VAR and Max-Share

This sections describes how the shocks in the proxy VAR can be disentangled using the Max-Share framework that was introduced by Faust (1998) and Uhlig (2004b). The key assumption behind the Max-Share approach is that the shock of interest j is the one that maximizes the contribution to the FEV of a target variable i over the considered horizon $\underline{h}$ up to $\overline{h}$. Then identification of the target shock amounts to finding the rotation vector q_j for which this maximum is achieved:

$$q_j^* = \text{argmax} \sum_{h=\underline{h}}^{\overline{h}} \Omega_{i,j}^z(h) \quad \text{s.t.} \quad q_j' q_j = 1. \tag{26}$$

The closed form solution of the baseline Max-Share maximization problem via the eigenvalues presented by Uhlig (2004b) also applies to the proxy VAR case in (27).

A key advantage of the Max-Share approach in the proxy VAR framework is that it does not require the assumption that the shock of interest is the one which maximizes the contribution to the FEV of a target variable among all possible shocks. The assumption reduces to the shock being the one which maximizes the contribution among the shocks related to the instruments. In practice the latter assumption is generally easier to defend depending on the empirical application. Yet, under which circumstances the Max-Share approach correctly identifies the shocks of interests is discussed in the next two subsections.

In the following I only consider the case when two shocks are identified with two instruments. In practice the case of two instruments is highly relevant, as finding multiple convincing proxy variables is difficult and finding two of them is already a challenging task. If two shocks are identified using two instruments the rotations matrix Q has dimension 2×2. Then identifying the first column of a 2×2 orthogonal matrix also identifies the second column up to a sign normalization due to the properties of orthonormal matrices:

$$Q = \begin{pmatrix} q_{11} & q_{12} \\ q_{21} & q_{22} \end{pmatrix}, \qquad 1 = q_{21}^2 + q_{22}^2 \quad \text{and} \quad 1 = q_{11}^2 + q_{12}^2. \tag{27}$$

The conditions of the 2×2 orthogonal matrices imply that each element of Q is

$-1 \leq q_{ij} \leq 1$. Further they imply that $q_{21} = \pm\sqrt{1-q_{11}^2}$, $q_{12} = \pm q_{21}$ and $q_{22} = \pm q_{11}$. Hence, everything can be written in terms of q_{11} up to sign normalizations. It follows that the identification of one shock via the Max-Share framework also gives the structural parameters of the second shock up to a sign normalization. Suppose, the first shock is identified with the Max-Share strategy, then the impulse responses of the second shock are pinned down up to sign. With more than two instruments the Max-Share approach does not immediately grant identification of the remaining shocks that are related to the instruments. Though, one rarely has more than two convincing instruments at hand.

3.2.1 Ruling out Confounders via the Proxy VAR

Rather recently Dieppe et al. (2019) highlighted that the key identification assumption of the Max-Share framework is violated if another shock also contributes to the FEV of the target variable. To give an example, assume that the technology shock is accountable for most of the FEV of a total factor productivity (TFP) measurement. If the technology shock is identified as the shock that maximizes the contribution to the TFP measurement, the results will be biased if also other shocks contribute to the FEV of the TFP measurement. Dieppe et al. (2019) present strategies how to circumvent this problem of confounding shocks in the baseline Max-Share identification without proxies. In this section I focus on the remedies to the bias concerns that the proxy VAR framework offers.

First and foremost, the proxy VAR helps with the confounding shocks as it rules out confounding shocks that are not related to the proxies. Proposition 3.2 formalizes this property of the Max-Share approach in the proxy VAR. The proof is relegated to the Appendix A.

Proposition 3.2. (Exclusive Contribution) Suppose two valid proxy variables z_1 and z_2 are available which are related to shocks w_1 and w_2. If $\Omega_{i,2}(h) = 0$ holds for $\underline{h} \leq h \leq \overline{h}$. Then

$$q_1^* = \text{argmax} \sum_{h=\underline{h}}^{\overline{h}} \Omega_{i,1}^z(h) \quad \text{s.t.} \quad q_1' q_1 = 1,$$

point identifies the shocks w_1 and w_1 up to a sign normalization.

Proposition 3.2 establishes that if out of the shocks that are related to the instruments one exclusively contributes to the FEV of the target variable, both shocks are correctly identified by the Max-Share framework. For example, assume two proxies are used to identify two shocks. One of the shocks contributes the most to the FEV of a specified variable and out of the two shocks that are related to the proxies it contributes exclusively to the FEV of this variable. Suppose another shock that is not related to the proxies also contributes to the FEV of this target variable. Yet, as it is not related to the proxies it is ruled out as a confounding shock. As out of the two shocks that are related to the proxies only one exclusively contributes to the FEV of the target variable, the Max-Share framework correctly disentangles and identifies both shocks of interest.

The case of exclusive contribution is a rather strict assumption which also offers the possibility to identify the shocks through imposing a recursive structure on the proxy impact matrix. Yet, the next subsection describes how the Max-Share approach can be employed without the assumption of exclusive contribution.

3.2.2 Tackling the Bias

If the assumption of exclusive contribution for one of the two identified shocks is not reasonable, additional inequality restrictions $IQ_{i,j,h}(q_{11})$ which augment the Max-Share framework can help to nevertheless correctly identify the true structural parameters. Proposition 3.3 states a sufficient condition under which the structural parameters are identified. The rotation matrix that corresponds to the true structural parameters is denoted by Q^* with its columns q_j^*. In the following I restrict the first element of Q, q_{11}, to be positive what simply helps with writing down the conditions for successful identification. In practice this means the shock is normalized to be an expansionary or contractionary - shock depending on the application - during the identification. Yet, after successful identification one can transform the shock into its contractionary/expansionary counterpart as usual by multiplying its respective column of the impact matrix or rotation matrix Q^* with -1.

Proposition 3.3. Let $q_{11} \in [0, 1]$. Suppose two valid proxy variables z_1 and z_2 are available which are related to shocks w_1 and w_2. Suppose out of w_1 and w_2, w_1 contributes the most, but not exclusively, to the FEV of variable i for $\underline{h} \leq h \leq \overline{h}$.

The augmented Max-Share approach

$$q_1^* = \text{argmax} \sum_{h=\underline{h}}^{\overline{h}} \Omega_{i,1}^z(h) \tag{28}$$

$$\begin{aligned}
&\text{s.t.} \\
&q_1' q_1 = 1, \\
&q_1' q_2 = 0, \\
&q_{11} \geq 0, \\
&IQ_{i,1,h}(q_{11}) \lesseqgtr \epsilon,
\end{aligned}$$

identifies the true structural parameters if

(a) $IQ_{i,1,h}(q_{11}) \lesseqgtr \epsilon$ implies a single binding linear restriction on q_{11} and

(b) the restrictions is set such that it implies $q_{11} \lesseqgtr q_{11}^*$.

The sign of ϵ and the direction of the inequality of the added constraint depends on the application. Whether condition (a) of Proposition 3.3 is satisfied depends on the type of inequality restriction that is placed while condition (b) requires the economic intuition behind the chosen restriction to be correct. In practice one can check whether condition (a) is satisfied and in the next paragraph I provide an example for two different types of inequality constraints. The implications of condition (b) will be discussed.

Proposition 3.4 gives a sufficient condition under which condition (a) of Proposition 3.3 is satisfied.

Proposition 3.4. Let $q_{11} \in [0, 1]$. Suppose a single linear restriction is placed on $IQ_{i,1,h}(q_{11})$. If $IQ_{i,1,h}(q_{11})$ is monotonic at $q_{11} \in [0, 1]$, $IQ_{i,1,h}(q_{11}) \lesseqgtr \epsilon$ implies a single linear restriction on q_{11} for $q_{11} \in [0, 1]$.

This paper considers two types of inequality restrictions $IQ_{i,1,h}(q_{11})$. Firstly, a standard sign restriction on the impulse response of the first shock on a specified variable for a single horizon h, i.e. $\eta_{i,1,h}(q_{11}) \lesseqgtr \epsilon$. The second constraint restricts the difference of the of impulse responses of the two identified shocks on a single variable i for a single horizon h, i.e. $D_{i,h}(q_{11}) = \eta_{i,1,h} - \eta_{i,2,h} \lesseqgtr \epsilon$, which translates to one shock having a larger impact than the other shock on the variable and horizon. The latter type of restriction adds another possibility to incorporate economic intuition into the identification. Checking whether the sufficient for condition (a) is satisfied boils down to checking whether $\eta_{i,1,h}(q_{11})$ or $D_{i,h}(q_{11})$ are monotonic at $q_{11} \in [0, 1]$.

Recall, that the structural impulse response of variable i to the first shock at horizon h is given by $\eta_{i,1,h} = e_i' C_h B_z q_1$, where e_i is the first column of the identity matrix I_2. Let

$$C_h B_z = \begin{pmatrix} \Theta_{1,1,h} & \Theta_{1,2,h} \\ \Theta_{2,1,h} & \Theta_{2,2,h} \\ \vdots & \vdots \\ \Theta_{k,1,h} & \Theta_{k,2,h} \end{pmatrix}.$$

To check whether $\eta_{i,1,h}(q_{11})$ is monotonic let Q^{max} be the rotation matrix obtained by the baseline Max-Share framework under the condition that $q_{11}^{max} \geq 0$. Let B_z^c be the one initial candidate for B_z, e.g. given by B_{11}^c. Then $\Theta_{i,1,h}$ and $\Theta_{i,2,h}$ can be computed with the reduced form parameters C_h and $B_z = B_z^c Q^{max}$. Recall that q_{11} is normalized to be positive and the according sign of q_{21} is obtained via the sign of q_{21}^{max}. If the signs of $\Theta_{i,1,h} q_{11}^{max}$ and $\Theta_{i,2,h} q_{21}^{max}$ are the opposite, $\eta_{i,1,h}(q_{11})$ is strictly monotonic at $q_{11} \in [0, 1]$. Note that $\eta_{i,1,h}(q_{11})$ is either strictly monotonic or not monotonic at all.

For the difference restriction $D_{i,h}(q_{11})$ the second column of Q has to be normalized such that $\eta_{i,1,h}$ and $\eta_{i,2,h}$ have the same sign. This ensures that $D_{i,h}(q_{11}) = \eta_{i,1,h} - \eta_{i,2,h}$ actually represents a difference and not the sum of the impulse responses. Recall that $q_{22} = \pm q_{11}$ and $q_{12} = \pm q_{21}$. Hence, the second column is only pinned down up to sign due to the first column of Q. As for the first shock the second column of Q is normalized such that it either represents an expansionary or contractionary shock in the identification. Converting it back into a the opposing shock after successful identification is described above based on the first shock.

Algorithm 3 describes how to do the necessary normalization of the second column and how to asses whether $D_{i,h}(q_{11})$ is monotonic given this normalization.

Algorithm 3.

1. Carry out the baseline Max-Share identification under the condition $q_{11} \geq 0$ and check whether q_{21}^{max} is positive or negative.

2. Get q_2 by setting $q_{22} = q_{11}^{max}$ and $q_{12} = -q_{21}^{max}$.

3. Compute $\eta_{i,1,h} = e_i' C_h B_z q_1$ and denote its sign.

4. Compute $\eta_{i,2,h} = e_i' C_h B_z q_2$. If $\eta_{i,2,h}$ has the opposite sign of $\eta_{i,1,h}$ change the sign normalization of q_2 (multiply it with -1).

5. Compute $\Theta_D = \Theta_{i,h,1} - \Theta_{i,h,2}$ and $\Theta_S = \Theta_{i,h,1} + \Theta_{i,h,2}$. Record the signs of the two quantities.

6.1 If q_{21}^{max} is positive and given q_2 from Step 4, $D_{i,h}(q_{11})$ is monotonic if:

(i) the signs of Θ_D and Θ_S are the same and $q_{22} = q_{11}^{max}$,

(ii) or if the signs Θ_D and Θ_S are the opposite and $q_{22} = -q_{11}^{max}$.

6.2 If q_{21}^{max} is negative and given q_2 from Step 4, $D_{i,h}(q_{11})$ is monotonic if:

(i) the signs of Θ_D and Θ_S are the same and $q_{22} = -q_{11}^{max}$,

(ii) or if the signs Θ_D and Θ_S are the opposite and $q_{22} = q_{11}^{max}$.

Details regarding algorithm 3 can be found in the appendix. Yet, monotonicity is just an easy to check sufficient condition for condition (a) to hold. Further details under which circumstances condition (a) is satisfied without monotonicity of $IQ_{i,1,h}(q_{11})$ can also be found in Appendix A.

Condition (b) of Proposition 3.3 requires the restriction to be set such that $q_{11} \lesseqgtr q_{11}^*$. For the simple sign restriction on the impulse responses this means that one response of the identified shock at one horizon has to be known. For the difference restriction one needs to gauge the difference in the responses of the shocks correctly, i.e. the true ϵ^* has to be known. In practice such knowledge has to be drawn from economic theory, previous results or pure economic intuition. The simulation study in section 4 illustrates the correct choice of ϵ such that condition (b) is satisfied.

Yet, if the true ϵ^* is unknown an inequality restriction can nevertheless help to reduce the bias. Let $\delta_{i,j,h} = \eta_{i,j,h}(q_{11}^*) - \eta_{i,j,h}(q_{11})$ be the bias of the structural impulse response of variable i at horizon h to shock j and $\epsilon^{max} = IQ_{i,j,h}(q_{11}^{max})$.

Proposition 3.5 (Reducing the Bias) Let $q_{11} \in [0,1]$. Suppose $IQ_{h,i,1}(q_{11})$ is continuous in q_{11} and $IQ_{h,i,1}(q_{11}) \gtreqless \epsilon$ implies a binding linear restriction on q_{11}. Let q_{11}^{res} be the implied restriction such that $q_{11} \gtreqless q_{11}^{res}$. If $\epsilon^{max} < \epsilon < \epsilon^*$ $(\epsilon^{max} > \epsilon > \epsilon^*)$ and $\eta_{i,j,h}(q_{11})$ is a strictly monotonic function at $q_{11} \in [q_{11}^{max}, q_{11}^*]$ $(q_{11} \in [q_{11}^*, q_{11}^{max}])$ the absolute bias $|\delta_{i,j,h}|$ decreases as $\epsilon^* - \epsilon$ $(\epsilon - \epsilon^*)$ decreases.

Example: Suppose the restriction is placed on $\eta_{1,1,0}(q_{11})$. *Let* $\eta_{1,1,0}(q_{11})$ *be a strictly monotonic function at* $q_{11} \in [0,1]$ *and let the true* $\eta_{1,1,0}^* = 1$. *With the unrestricted Max-Share approach one gets* $\eta_{1,1,0}^{max} = 1.5$. *The correct inequality constraint would be* $\eta_{1,1,0}(q_{11}) \leq 1$, *yet if this is unknown the researcher might choose* $\eta_{1,1,0}(q_{11}) \leq 1.2$ *or* $\eta_{1,1,0}(q_{11}) \leq 1.1$. *As* $\eta_{1,1,0}(q_{11})$ *is strictly monotonic the bias of* $\eta_{1,1,0}$ *is smaller for the constraint with* 1.1 *compared to* 1.2 *as* 1.1 *is closer to the true* ϵ^*. *However, if the researcher picks* $\eta_{1,1,0}(q_{11}) \leq 0.9$ *the bias increases again and it could be larger compared to the constraints with* 1.1 *or* 1.2 *depending on the* *functional form of* $\eta_{1,1,0}(q_{11})$.

Hence, approaching ϵ^* from ϵ^{max} reduces the bias. Yet, if one overshoots and i.e. $\epsilon^{max} < \epsilon^* < \epsilon^{res}$ the bias increases. Hence, if the true ϵ^* is unknown a more conservative choice of ϵ guarantee a reduction of the bias under the condition described in Proposition 3.4. The simulation study in the next section illustrates how the bias changes for different choices of ϵ.

Checking whether the bias is guaranteed to decrease, firstly requires to check whether condition (a) of Proposition 3.3 is fulfilled for the imposed constraint. Second, one has to check whether for the variable and horizon of interest $\eta_{i,1,h}(q_{11})$ is strictly monotonic over the relevant domain $q_{11} \in [q_{11}^{max}, q_{11}^*]$. If $\eta_{i,1,h}(q_{11})$ is strictly monotonic at $q_{11} \in [0, 1]$ it is also strictly over the relevant domain. Otherwise one can check whether $\eta_{i,1,h}(q_{11})$ is strictly monotonic at $q_{11} \in [q_{11}^{max}, 1]$ or $q_{11} \in [0, q_{11}^{max}]$ depending on whether the restriction implies $q_{11}^{res} \geq q_{11}^{max}$ or $q_{11}^{res} \leq q_{11}^{max}$. Note that for the second shock on has to check whether $CB_{i,h,1}q_{12}^{max}$ and $CB_{i,h,2}q_{22}^{max}$ have opposite signs in order to determine whether $\eta_{i,2,h}(q_{11})$ is strictly monotonous or not.

In practice one can also report results for different values of ϵ over a range of values one is confident that ϵ^* is contained. This however de-sharpens the identification the larger the range of ϵ values. Thus the augmented Max-Share approach is most useful when a rather strong intuition for the correct ϵ^* exists.

3.2.3 Estimation and Inference

The combination of the proxy VAR with the Max-Share framework can also be handled with the Bayesian Algorithm 1 described in Section 3.1. In combination with the Max-Share framework, steps 2 and 3 are simply replaced with carrying out the Max-Share optimization. Note that this reduces the robust Bayesian approach to conventional Bayesian inference. Step three in Algorithm 1, the core of the robust Bayesian inference, computes the boundaries of the identified set and in the point identification case the identified set is a singleton. Hence, computing the bounds reduces to the computation of the point estimate.

However, in point identification scheme bootstrap inference is popular. In this case, I propose the bootstrap by Jentsch and Lunsford (2022), which is based on the heteroskedasticity robust bootstrap by Brüggemann, Jentsch, and Trenkler (2016). This approach relies on estimating Z and Σ to get an estimate for B_{11}^c (see e.g. Piffer & Podstawski, 2018). The bootstrap confidence intervals are constructed in the conventional way.

4 Simulation Results

The simulation study of this section serves the purpose of illustrating the Max-Share identification in the presence of two proxies. It illustrates the flaw in the baseline Max-Share approach and how the additional inequality constraint can be used as a remedy.

I simulate a trivariate system following Piffer and Podstawski (2018) who use the New Keynesian model by An and Schorfheide (2007) and Komunjer and Ng (2011). The model contains interest rates r_t, output x_t and inflation π_t. TFP shocks w_t^z, government spending shocks w_t^g and monetary shocks w_t^r are the structural shocks that hit the system. As pointed out by Giacomini (2013), calibrating the parameter gives the following DGP:

$$\begin{pmatrix} r_t \\ x_t \\ \pi_t \end{pmatrix} = \begin{pmatrix} 0.79 & 0 & 0.25 \\ 0.19 & 0.95 & -0.46 \\ 0.12 & 0 & 0.62 \end{pmatrix} \begin{pmatrix} r_{t-1} \\ x_{t-1} \\ \pi_{t-1} \end{pmatrix} + \begin{pmatrix} 0.61 & 0 & 0.69 \\ 1.49 & 1 & -1.16 \\ 1.49 & 0 & -0.75 \end{pmatrix} \begin{pmatrix} w_t^z \\ w_t^g \\ w_t^r \end{pmatrix}. \tag{29}$$

In contrast to Piffer and Podstawski (2018) I set the variance of the structural shocks to unity in order easily compute the actual contribution to the FEV decomposition. Hence, the structural shocks are drawn from a normal distribution with mean zero and unit variance and then used to simulate the data with equation (30). The instruments are constructed with:

$$\begin{aligned} m_{1t} &= \tau_1 w_t^z + (1-\tau_1) w_t^{(2)} + \tau_2 \nu_{1t} \\ m_{2t} &= (1-\tau_1) w_t^z + \tau_1 w_t^{(2)} + \tau_2 \nu_{2t}, \end{aligned}$$

where τ_1 governs the strength of the relation of the first to shocks with the instruments and τ_2 governs the effect of the white noise disturbances ν_{1t} and ν_{2t}. I set $\tau_1 = 0.55$ and $\tau_2 = 0.01$ which leads to the proxies being sufficiently strong. The instruments are related to the respective structural shocks depending on the scenarios which are described below, i.e. $w_t^{(2)}$ will either be w_t^g or w_t^r.

The technology shock w_t^z is accountable for the most part of the FEV of the interest rate r_t. Up to horizon $H = 13$ the technology shock w_t^z contributes on average 82% to the FEV of the interest rate r_t. The government spending shock w_t^g does not contribute to the FEV and the monetary policy shock w_t^r contributes the remaining 18%. In this section the interest rate is always the target variable in the Max-Share framework. Hence, the underlying assumption is that the technology shock is the one that maximizes the contribution to the FEV of the interest rate. An interesting feature of this DGP is that the government spending shock does not

Table 1: Two Shocks without Exclusive Contribution

DGP		Proxy + Max-Share		Proxy + Cholesky	
Scenario A					
0.61	0	0.609 (0.007)	0.004 (0.004)	0.609 (0.007)	0 (0)
1.49	1	1.487 (0.016)	1.014 (0.036	1.485 (0.012)	1.004 (0.03)
1.49	0	1.488 (0.008)	0.015 (0.008)	1.488 (0.008)	0.004 (0.023)
Scenario B					
0.61	0.69	0.766 (0.008)	0.512 (0.004)	0.921 (0.006)	0 (0)
1.49	-1.1	1.161 (0.021)	1.624 (0.019	0.163 (0.022)	1.845 (0.016)
1.49	-0.75	1.25 (0.016)	1.578 (0.014)	0.426 (0.017)	1.6131 (0.011)

The table depicts the average of the estimated structural parameters over the 1,000 Monte-Carlo simulation iterations derived with the proxy VAR. The shocks are once disentangled with the baseline Max-Share approach and once with the Cholesky decomposition. The value in the parenthesis depicts the respective standard deviation.

contribute to the FEV of the interest rate and inflation at any horizon. This enables me to construct two scenarios:

Scenario A: The proxies are constructed such that they are related to the technology shock w_t^z and the government spending shock w_t^g. Out of these two shocks w_t^z contributes exclusively to the FEV of the interest rate r_t.

Scenario B: The proxies are constructed such that they are related to the technology shock w_t^z and the monetary policy shock w_t^r. Both these two shocks contribute to the FEV of the interest rate r_t.

4.1 Simulation Results - Max-Share

This subsection presents the simulation results for the case when to shocks are disentangled in the proxy VAR. The first results compare Scenario A and B which are described above.

Table 1 depicts the results for the identification via maximization of the FEV after incorporating the information of the instruments as in (26) and without further inequality restrictions on relative magnitudes. As this is more of a confirmation exercise in which cases the Max-Share approach succeeds and fails I choose a large sample size of $T = 1,000$ with $M = 1,000$ Monte-Carlo iterations. The first two columns of the table show the true structural parameters of the DGP, the next two columns the combination of proxy VAR and Max-Share and the last two the identification via the Cholesky decomposition as in e.g. Mertens and Ravn (2013), i.e. $B_{11} = B_{11}^c$ is lower triangular. Looking at the results for Scenario A shows that after incorporating the proxies the shock that is not related to them is purged from the maximization problem. Only the two shocks that are related to the instruments are factored in and as one of the shocks contributes exclusively to the FEV of the target variable the Max-Share approach is suitable to disentangle these two. Yet, this set-up with exclusive contribution implies a recursive structure for the contemporaneous impacts of the shock, and thus the Cholesky decomposition for the upper 2×2 block of the proxy impact matrix will also identify the true underlying structural parameters.

Hence, the potentially more interesting case is when both identified shocks contribute to the FEV of the target variable as in Scenario B. As seen in the panel for Scenario B of Table 1, the Cholesky decomposition fails to identify the true impact matrix as there is no recursive structure between the two identified shocks. However, as expected also the combination of the proxy VAR with the Max-Share approach yields biased results because both shocks contribute to the FEV of the target variable. As pointed out by Dieppe et al. (2019), the Max-Share framework will be biased due to the confounding shock.

To successfully disentangle the two shocks when both shocks contribute to the FEV, the Max-Share framework needs to be augmented. In this case I use an inequality constraint which restricts the difference in the contemporaneous responses of output $D_{2,0}$. In this DGP, a common, one standard deviation, expansionary technology shock has a more pronounced positive effect (1.49) than a common expansionary monetary policy shock (1.1). Augmenting the maximization problem such that this inequality constraint holds helps to disentangle the two shocks.

If the conditions of Proposition 3.3 hold, identification of the true underlying shocks is guaranteed. Algorithm 3 is used to normalize the second column such that $D_{2,0}(q_{11})$ is a monotonic function at $q_{11} \in [0, 1]$, and thus a linear restriction on it implies a linear restriction on q_{11}.

1. Carrying out the unrestricted Max-Share approach with $q_{11}^{max} \geq 0$ gives $q_{21}^{max} \geq 0$.

2. Set $q_{22} = q_{11}^{max} \geq 0$ and $q_{12} = -q_{21}^{max} \geq 0$

3. $\eta_{2,1,0} = 1.161 \geq 0$.

4. $\eta_{2,2,0} = 1.612 \geq 0$.

5. $\Theta_D \leq 0$ and $\Theta_S \geq 0$.

Table 2: Max-Share with Additional Inequality Constraint - Scenario B

DGP		Max-Share^{+}, T=1000		Max-Share^{+}, T=250	
Panel A: $\epsilon = 0.38$					
0.61	0.69	0.613 (0.029)	0.688 (0.026)	0.612 (0.057)	0.688 (0.052)
1.49	-1.1	1.486 (0.044)	-1.106 (0.044)	1.481 (0.087)	-1.101 (0.087)
1.49	-0.75	1.487 (0.031)	-0.755 (0.038)	1.483 (0.062)	-0.755 (0.075)
Panel B: $\epsilon = 0.2$					
0.61	0.69	0.659 (0.027)	0.644 (0.027)	0.658 (0.055)	0.643 (0.054)
1.49	-1.1	1.406 (0.044)	-1.206 (0.045)	1.405 (0.075)	-1.205 (0.074)
1.49	-0.75	1.432 (0.032)	-0.856 (0.037)	1.429 (0.062)	-0.858 (0.072)
Panel C: $\epsilon = 0$					
0.61	0.69	0.706 (0.026)	0.592 (0.027)	0.706 (0.053)	0.591 (0.055)
1.49	-1.1	1.311 (0.037)	-1.311 (0.037)	1.31 (0.075)	-1.309 (0.074)
1.49	-0.75	1.362 (0.032)	-0.963 (0.036)	1.36 (0.063)	-0.965 (0.07)

The table depicts the average of the estimated structural parameters over the 1,000 Monte-Carlo simulation iterations. The estimates are derived with the Max-Share^{+} framework in the proxy VAR with different values of ϵ.

6. From the reduced form parameter one gets $DC_{2,0} \leq 0$ and $SC_{2,0} \geq 0$.

3.1 As the signs of $DC_{2,0}$ and $SC_{2,0}$ are the opposite the second column has to be normalized such that $q_{22} = q_{11} \geq 0$ and $q_{12} = -q_{12} \leq 0$.

With these normalizations the contemporaneous response of output to the technology shock is $\eta_{2,1,0} = 1.161$ while the response to the monetary shock is $\eta_{2,2,0} = 1.612$ in the unrestricted Max-Share framework. Hence, $D_{2,0} = \eta_{2,1,0} - \eta_{2,2,0}$ is an actual difference as the signs of the two responses are the same. Knowing the DGP makes it easy also fulfil condition (b) of Proposition 3.3 by placing the constraint $D_{2,0} \geq \epsilon = 0.39$, which is a binding constraint. In order to impose such a constraint, one would need to argue that from prior knowledge or economic theory it is known that the common expansionary technology shock affects output more than the common expansionary monetary policy shock on impact. Without knowledge about the true DGP the true margin ϵ^* is typically unknown and needs to be gauged by the researcher. This simulation exercise reports results for different values of ϵ.

The full maximization problem for this particular simulation with the just mentioned restrictions is:

$$q_1^* = \text{argmax} \sum_{h=0}^{H} \Omega_{1,1}^{z}(h) \tag{30}$$

$$\begin{aligned}
&\text{s.t.} \\
&q_1' q_1 = 1, \\
&q_1' q_2 = 0, \\
&\eta_{2,1,0} - \eta_{2,2,0} \geq \epsilon, \\
&q_{11} \geq 0, \\
&q_{22} \geq 0.
\end{aligned}$$

Table 2 depicts the results for this augmented Max-Share identification, denoted by Max-Share$^+$. The first two columns again depict the true DGP parameters, while columns three and four give the results of the Max-Share$^+$ framework with $T = 1,000$ while the last two columns give the results for $T = 250$. Panel A shows the results for $\epsilon = 0.38$ which is very close to the true margin by which $\eta_{2,1,0}$ exceeds $\eta_{2,2,0}$ in absolute terms. Panel B shows the results for $\epsilon = 0.2$ and Panel C the results for $\epsilon = 0$. The latter represents the case when restriction boils down to a sign restriction on the relative magnitudes of the two shocks.

Comparing the estimates throughout the panels reveals that having the (almost) correct economic intuition with the inequality restriction ($\epsilon = 0.38$) removes almost all of the bias of the Max-Share approach. Yet, if the true margin is not met part of the bias remains and it is larger the less close the true margin is met. This is true for both the technology as well as the monetary policy shock. Comparing the results in terms of the sample sizes shows that also for smaller sample sizes like $T = 250$ the correct identification is achieved. Naturally, the bias also remains for smaller sample sizes when ϵ is not very close to the true margin.

Figure 1 and 2 show the 2.5% and 97.5% quantiles (dashed lines) of the estimated impulse responses identified by the augmented Max-Share throughout the 1,000 Monte-Carlo simulation rounds. The true impulse responses are depicted by the solid lines. Figure 1 presents the responses obtained with the $\epsilon = 0.38$, close to the true margin while Figure 2 presents the results for $\epsilon = 0$. The impulse responses for $\epsilon = 0.2$ can be found in the Appendix B.

Figure 1: 95% Point Estimate Bands, $\epsilon = 0.38$ - Scenario B

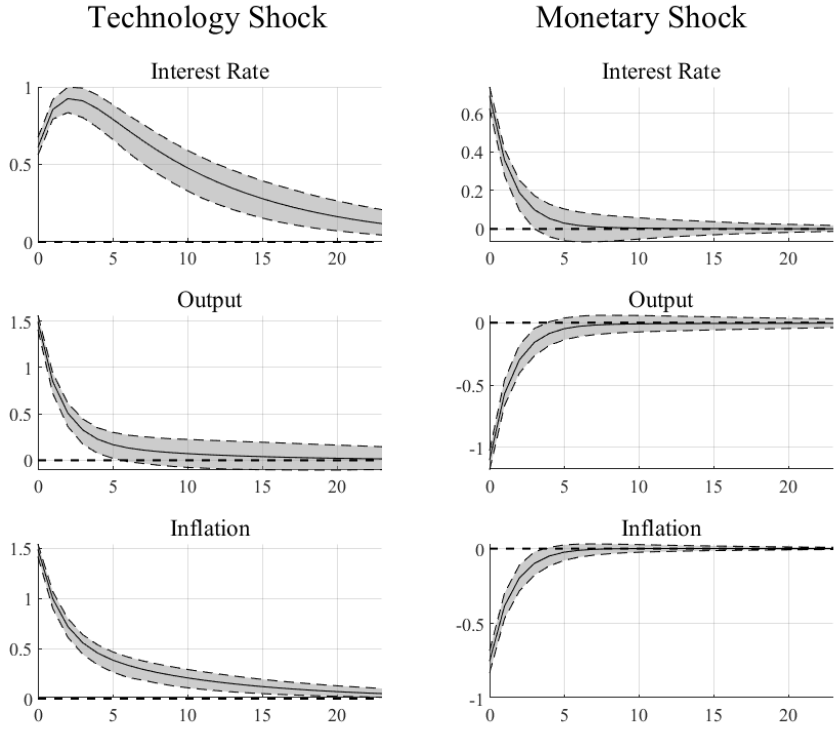

The solid lines depict the true impulse responses of the DGP. The dashed lines are the 2.5% and 97.5% quantile of the solutions found for the 1,000 Monte-Carlo simulation iterations.

The figures are in line with the results of Table 2. The estimated responses in Figure 1 closely identify the true structural impulse response parameters while the responses in Figure 2 reflect the bias of the impact matrix parameters in the bias of the impulse responses especially at earlier horizons.

The bias of the structural impulse responses at different horizon and for different values of ϵ is depicted in Table 3 for the technology shock and in Table 4 for the monetary policy shock. Comparing the results along the columns shows that the bias is typically larger the further away ϵ is from ϵ^* and for earlier horizons of the responses. These patterns are consistent throughout both tables, and therefore both identified shocks. Results for $T = 250$ are presented to the Appendix B.

The patterns found in Tables 3 and 4 are visualized in Figures 3 and 4. The coloured lines depict the bias of the structural impulse responses at different horizons and for different values of ϵ. Comparing the results throughout the panels the bias is larger when ϵ is farther away from the true margin. This indicates that the condition of Proposition 3.6 is most likely fulfilled for most of the responses throughout the variables, shocks and horizons. Only the responses of output to the monetary policy shock $\eta_{2,2,h}$ for some horizons hint towards some non-monotonic functions. The same

Figure 2: 95% Point Estimate Bands, $\epsilon = 0$ - Scenario B

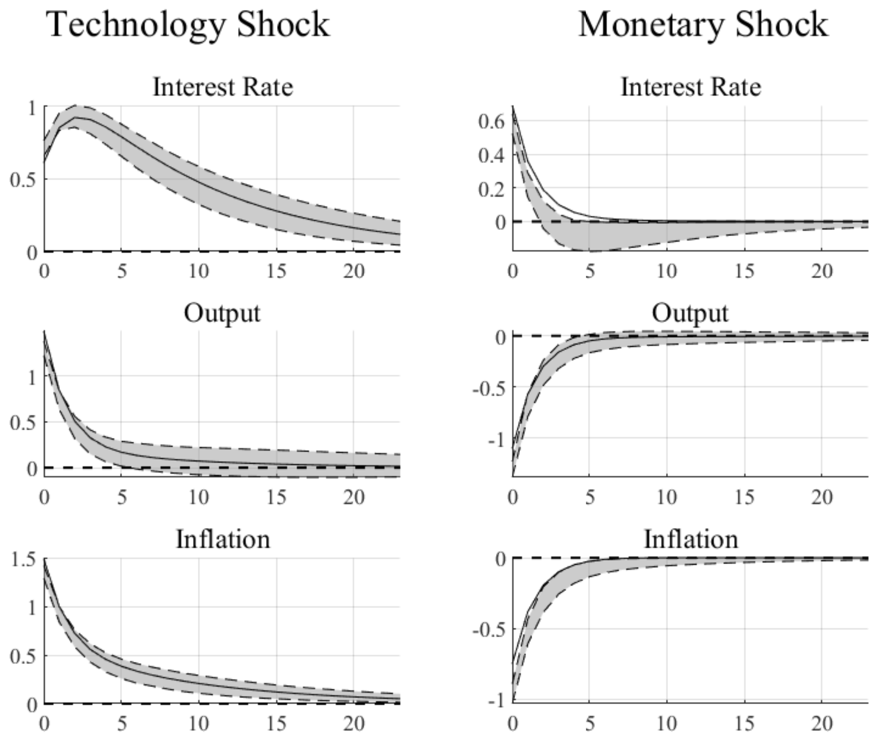

The solid lines are the true impulse responses of the DGP. The dashed lines are the 2.5% and 97.5% quantile of the solutions found for the 1,000 Monte-Carlo simulation iterations.

visualization for $T = 250$ is again relegated to the Appendix B.

Lastly, the additional constraints in the maximization problem (30) can also serve a pure inequality restrictions in order to set identify the shocks. For example, one could also try to disentangle the shocks in the proxy VAR with this inequality restrictions alone without the Max-Share framework. Figure 11 of the Appendix B depicts the point identified impulse responses derived with the maximization problem in (30) and also the identified set of the impulse responses when only the inequality restriction is used. The figure shows that the use of the Max-Share framework helps to estimate the structural impulse responses more precisely, as the simulated sets from identification with only inequality restrictions are rather wide compared to the range of simulated point estimates of the augmented Max-Share approach for the majority of the impulse responses. Hence, incorporating the economic intuition behind the constraint into the Max-Share framework yields sharper identification compared to using only the inequality restriction.

Table 3: Bias of the IRFs, $T = 1000$ - Scenario B

Variable	$h = 0$	$h = 6$	$h = 12$	$h = 18$
Technology Shock with $\epsilon = 0.38$				
r_t	0.0025	-0.0178	-0.0198	-0.0136
x_t	-0.0045	-0.0108	-0.0055	-0.0018
π_t	-0.0026	-0.0146	-0.0113	-0.0065
Technology Shock with $\epsilon = 0.2$				
r_t	0.0486	-0.0186	-0.0207	-0.014
x_t	-0.0844	-0.0131	-0.0061	-0.0022
π_t	-0.0584	-0.0163	-0.0117	-0.0067
Technology Shock with $\epsilon = 0$				
r_t	0.0958	-0.0233	-0.0235	-0.0154
x_t	-0.1795	-0.016	-0.0068	-0.0025
π_t	-0.1273	-0.0199	-0.0129	-0.0072
Monetary Shock with $\epsilon = 0.38$				
r_t	-0.0021	-0.0059	-0.0025	-0.0008
x_t	-0.0055	-0.0005	0.0009	0.001
π_t	-0.0051	-0.0029	-0.0007	-0.0001
Monetary Shock with $\epsilon = 0.2$				
r_t	-0.0462	-0.0546	-0.0278	-0.0138
x_t	-0.1056	-0.0088	-0.0025	-0.0007
π_t	-0.1062	-0.0249	-0.0115	-0.0057
Monetary Shock with $\epsilon = 0$				
r_t	-0.0982	-0.1084	-0.0557	-0.0282
x_t	-0.2105	-0.0184	-0.0067	-0.0029
π_t	-0.2135	-0.0491	-0.0234	-0.0119

The table depicts the average bias in the estimated structural parameters over the 1,000 Monte-Carlo simulation iterations. The estimates are derived with the Max-Share$^+$ framework in the proxy VAR with different values of ϵ.

Figure 3: Bias of the IRFs to the Technology Shock, $T = 1000$ - Scenario B

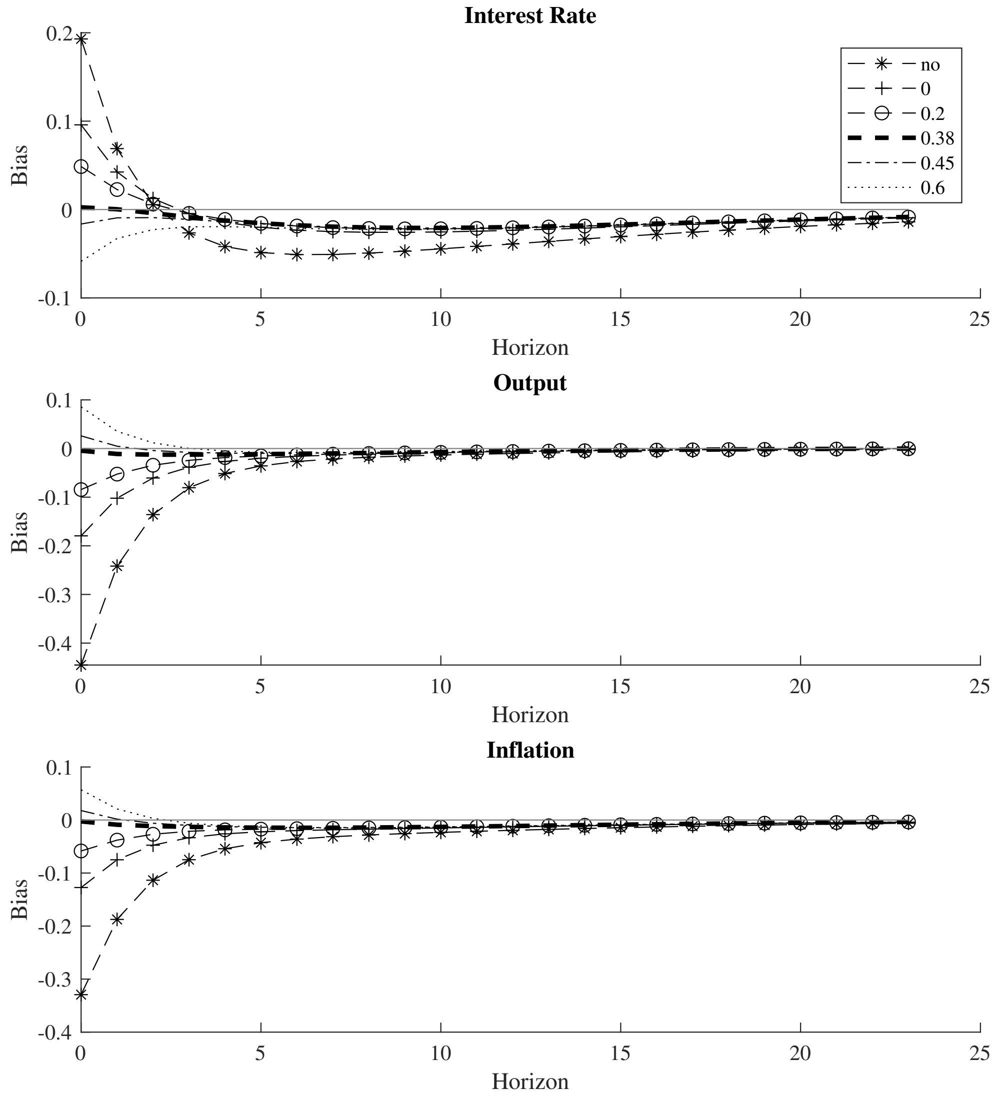

The different lines depict the average bias of the impulse response functions over 1,000 Monte-Carlo simulations for different values of ϵ.

Figure 4: Bias of the IRFs to the Monetary Shock, $T = 1000$ - Scenario B

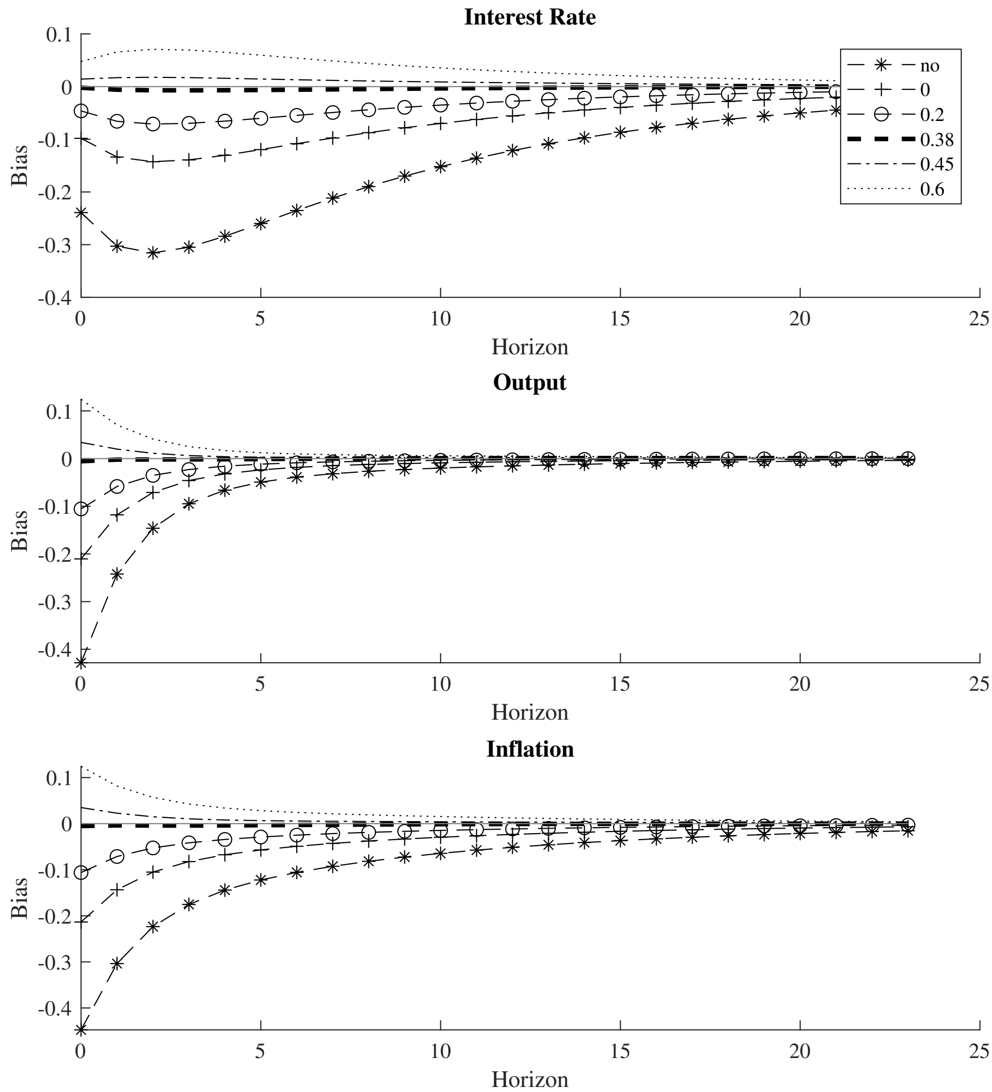

The different lines depict the average bias of the impulse response functions over 1,000 Monte-Carlo simulations for different values of ϵ.

5 Conclusion

Identifying restrictions on the FEV can be used in multiple ways to disentangle the shocks in the proxy VAR framework. Firstly, bounds the FEV as introduced by Volpicella (2022) replace or accompany other inequality restrictions to disentangle the shocks in the proxy VAR. This paper provides the general framework of the bounds applied to the proxy VAR and how to conduct robust Bayesian inference in this setting.

Second, the structural parameters are sharply point identified in the proxy VAR with the help of the Max-Share framework. For this approach the paper only considers the, in practice highly relevant, case of two shocks being identified using two instruments. I state under which condition the Max-Share approach successfully identifies the structural shock. If the baseline Max-Share approach suffers from bias due to confounding shocks an augmentation with an inequality constraint helps to remove or reduce the bias. I provide sufficient conditions under which the inequality constraint successfully removes or reduces the bias. In this paper I illustrate how to assess these conditions for two candidates of inequality constraints - for an inequality constraint on one impulse response at one horizon and for a constraint on the difference of impulse responses of two shocks on a specified variable. Further, I also provide guidance how to conduct inference for the Max-Share identification strategy in proxy VARs.

A simulation study highlights the intricacies of the Max-Share framework and illustrates how to assess the formal conditions for a successful Max-Share identification. Further, it illustrates the behavior of the bias when the sufficient conditions are not satisfied.

References

An, S., & Schorfheide, F. (2007). Bayesian Analysis of DSGE models. *Econometric Reviews*, *26*(2-4), 113-172.

Barsky, R. B., & Sims, E. R. (2011). News shocks and business cycles. *Journal of Monetary Economics*, *58*(3), 273-289.

Baumeister, C., & Hamilton, J. D. (2015). Sign restrictions, structural vector autoregressions, and useful prior information. *Econometrica*, *83*(5), 1963–1999.

Ben Zeev, N., & Pappa, E. (2017). Chronicle of a War Foretold: The Macroeconomic Effects of Anticipated Defence Spending Shocks. *The Economic Journal*, *127*(603), 1568-1597.

Brüggemann, R., Jentsch, C., & Trenkler, C. (2016). Inference in VARs with conditional heteroskedasticity of unknown form. *Journal of Econometrics*, *191*(1), 69-85.

Dieppe, A., Neville, F., & Kindberg-Hanlon, G. (2019). *New Approaches to the Identification of Low-Frequency Drivers: An Application to Technology Shocks.* The World Bank.

Faust, J. (1998). The robustness of identified VAR conclusions about money. *Carnegie-Rochester Conference Series on Public Policy*, *49*, 207-244.

Francis, N., Owyang, M. T., Roush, J. E., & DiCecio, R. (2014). A Flexible Finite-Horizon Alternative to Long-Run Restrictions with an Application to Technology Shocks. *The Review of Economics and Statistics*, *96*(4), 638-647.

Gertler, M., & Karadi, P. (2015). Monetary Policy Surprises, Credit Costs, and Economic Activity. *American Economic Journal: Macroeconomics*, *7*(1), 44-76.

Giacomini, R. (2013). The relationship between DSGE and VAR models. In *Advances in econometrics* (Vol. 32, p. 1-25).

Giacomini, R., Kitagawa, T., & Read, M. (2022). Robust Bayesian inference in proxy SVARs. *Journal of Econometrics*, *228*(1), 107-126.

Jentsch, C., & Lunsford, K. G. (2022). Asymptotically Valid Bootstrap Inference for Proxy SVARs. *Journal of Business & Economic Statistics*, *40*(4), 1876-1891.

Kilian, L., & Lütkepohl, H. (2017). *Structural vector autoregressive analysis.* Cambridge University Press.

Komunjer, I., & Ng, S. (2011). Dynamic identification of dynamic stochastic general equilibrium models. *Econometrica*, *79*(6), 1995–2032.

Lakdawala, A. (2019). Decomposing the effects of monetary policy using an external instruments SVAR. *Journal of Applied Econometrics*, *34*(6), 934-950.

Mertens, K., & Ravn, M. O. (2013). The Dynamic Effects of Personal and Corporate Income Tax Changes in the United States. *American Economic Review*, *103*(4), 1212-47.

Montiel Olea, J. L., & Nesbit, J. (2021). (Machine) learning parameter regions. *Journal of Econometrics*, *222*(1, Part C), 716-744.

Piffer, M., & Podstawski, M. (2018). Identifying Uncertainty Shocks Using the Price of Gold. *The Economic Journal*, *128*(616), 3266-3284.

Stock, J., & Watson, M. (2012). Disentangling the Channels of the 2007-2009 Recession. *Brookings Papers on Economic Activity*, *Spring 2012*, 81-135.

Uhlig, H. (2004a). Do technology shocks lead to a fall in total hours worked? *Journal of the European Economic Association*, *2*(2-3), 361-371.

Uhlig, H. (2004b). *What moves GNP?* (Econometric Society 2004 North American Winter Meetings No. 636).

Volpicella, A. (2022). SVARs Identification Through Bounds on the Forecast Error Variance. *Journal of Business & Economic Statistics*, *40*(3), 1291-1301.

A Appendix A

Proof of Proposition 3.1

The proof of Proposition 3.1 closely follows the ideas of the proof for Proposition 3.1 in the article by Volpicella (2022). The contribution of shock j to the FEV of variable i at horizon h is given by:

$$\Omega_{i,j}(h) = q_j' R_{i,h} q_j, \tag{31}$$

where $R_{i,h}$ is a positive semidefinite symmetric $l \times l$ real matrix. As $R_{i,h}$ is symmetric it can be diagonalized such that:

$$P' R_{i,h} P = D, \tag{32}$$

where P is an orthogonal matrix and D a diagonal matrix with the real eigenvalues λ_m^{ih} of matrix $R_{i,h}$ as entries on the diagonal for $m = 1, ..., l$.

The rest of the proof follows from the proof of Proposition 3.1 by Volpicella (2022).

■

To aid with the proof of Proposition 3.2 I first define under which conditions a shock does not contribute to the FEV of a specified variable.

Definition 1: Let C_i^h be the i-th row of the moving average coefficient matrix C_h and B_j^z the j-th column of the proxy impact matrix B_z. Shock j does not contribute to the FEV of variable i at horizon $\overline{h}$ if $C_i^h B_j^z = 0 \; \forall \; h \leq \overline{h}$.

As C_0 is just the identity matrix I_k, C_i^0 is just a row of I_k. Hence, under Definition 1 the i-th element of B_j^z has to be zero.

Example: Consider the case with two instruments in a three variable system. The second shock does not contribute to the FEV of the first variable. Definition 1 requires the B_z to have the following structure:

$$B_z = \begin{pmatrix} * & 0 \\ * & * \\ * & * \end{pmatrix}.$$

Proof of Proposition 3.2.

Suppose the two proxies z_1 and z_2 are valid and satisfy conditions (9) of the main text. Hence, the proxy VAR alone will identify the true proxy impact matrix B_z

up to a rotation with an orthonormal matrix Q. For simplicity and w.l.o.g. assume that the initial rotation matrix Q is just the identity matrix such that B_{11}^c is the Cholesky decomposition of $B_{11} = \Sigma_{11} - B_{12}B_{12}'$. Furthermore, w.l.o.g assume that the first two shocks of the system are related to the proxy variable and that the second shock does not contribute to the FEV of the first variable over the horizon $\underline{h}$ up to $\overline{h}$. Definition 1 requires the structure of the proxy impact matrix to be:

$$B_z = \begin{pmatrix} * & 0 \\ * & * \\ \vdots & \vdots \\ * & * \end{pmatrix}.$$

As the first variable contributes exclusively to the FEV of the first variable, the Max-Share approach maximizes the contribution of the first shock to the FEV of the first variable.

Recall that the contribution of the first shock to the FEV of the first variable at horizon h can be written as:

$$\Omega_{1,1}(h) = q_1' R_{1,h} q_1. \tag{33}$$

Uhlig (2004b) shows that the sum over all $\Omega_{1,1}(h)$ from horizons $\underline{h}$ up to $\overline{h}$ can be expressed by:

$$\sum_{h=\underline{h}}^{\overline{h}} \Omega_{1,1}^z(h) = q_1' S q_1, \tag{34}$$

where

$$S = \sum_{h=0}^{\overline{h}} (\overline{h} + 1 - \max(\underline{h}, h))(e_1 C_h B_z)'(e_1 C_h B_z) = \sum_{h=0}^{\overline{h}} (\overline{h} + 1 - \max(\underline{h}, h)) S_h, \tag{35}$$

with e_1 being the first row of the identity matrix I_k. Hence, $e_1 C_h B_z$ is just the first row of $C_h B_z$.

For $h = 0$, C_0 is just the identity matrix, and $e_1 C_0 B_z = (* \; 0)$, and thus

$$S_0 = \begin{pmatrix} * & 0 \\ 0 & 0 \end{pmatrix}.$$

If $h > 0$, due to Definition 1, $e_1 C_h B_z = (* \; 0)$ for $h < \overline{h}$, and thus

$$S_h = \begin{pmatrix} * & 0 \\ 0 & 0 \end{pmatrix} \quad \forall \; h < \overline{h}.$$

As S is just the weighted sum over all S_h,

$$S = \begin{pmatrix} * & 0 \\ 0 & 0 \end{pmatrix}.$$

Uhlig (2004b) shows that finding the rotation vector q_1^* that maximizes the sum over the contributions

$$q_1^* = \text{argmax } q_1' S q_1 \quad \text{s.t.} \quad q_1' q_1 = 1 \tag{36}$$

amounts to finding the eigenvector associated with the largest eigenvalue of the matrix S. Due to the particular structure of the matrix S induced by the exclusive contribution it can easily be seen that the eigenvector associated with the non-zero eigenvalue is just the first column of the identity matrix I_2. Hence, the rotation matrix Q^* is just the identity matrix I_2 up to a sign normalization of the columns. Thus, the maximum of the contribution to the FEV is achieved at the true proxy impact matrix parameters up to a sign normalization of the columns.

■

This paragraph aims to illustrate that Proposition 3.2 also holds without the assumption that B_{11}^c is the Cholesky decomposition of $B_{11} = \Sigma_{11} - B_{12}B_{12}'$. If another solution to $B_{11} = \Sigma_{11} - B_{12}B_{12}'$ is chosen, it can be represented as a rotation of B_z with an initial rotation matrix Q_{init}:

$$B_{init} = B_z Q_{init} = \begin{pmatrix} b_{11} & 0 \\ b_{21} & b_{22} \\ \vdots & \vdots \\ b_{k1} & b_{k2} \end{pmatrix} \begin{pmatrix} q_{11} & q_{12} \\ q_{21} & q_{22} \end{pmatrix}.$$

Again suppose that the first two shocks are the target shocks, from which the first shocks exclusively contributes to the FEV of the first variable. For $\underline{h} = \overline{h} = 0$ it can be nicely seen that in the process of the Max-Share optimization the initial rotation simply is reverted.

The first row of the rotated proxy impact matrix is $(b_{11}q_{11} \; b_{11}q_{12})$, and thus for $\underline{h} = \overline{h} = 0:$

$$S = \begin{pmatrix} b_{11}^2 q_{11}^2 & b_{11}^2 q_{11} q_{12} \\ b_{11}^2 q_{11} q_{12} & b_{11}^2 q_{12}^2 \end{pmatrix}.$$

It can be shown that the eigenvalues of S are $[b_{11}^2, 0]$ and a corresponding eigenvector to the non-zero eigenvalue is

$$q_1^* = \begin{pmatrix} q_{11} \\ q_{12} \end{pmatrix}.$$

Hence, the optimal rotation matrix due to the Max-Share identification is equal to the transposed initial rotation Q'_{init}, up to a sign normalization of the columns. Thus, the initial rotation is reverted as

$$B_{init} = B_z Q_{init} Q'_{init} = B_z \tag{37}$$

and the true impact matrix parameters are identified. Again, up to a sign normalization of the columns.

Proof of Proposition 3.3

Let $q_{11} \in [0, 1]$. Without loss of generality assume that the first shock is the target shock in the maximization of the Max-Share approach. In general the maximization problem of the Max-Share framework can be written as:

$$q_1^* = \text{argmax } q_1' S q_1 \quad \text{s.t.} \quad q_1' q_1 = 1, \tag{38}$$

where S is defined above and is a symmetric and positive semi definite matrix. Let:

$$S = \begin{pmatrix} s_{11} & s_{21} \\ s_{21} & s_{22} \end{pmatrix} \quad \text{and} \quad q_1 = \begin{pmatrix} q_{11} \\ q_{21} \end{pmatrix},$$

where $q_{21} = \pm\sqrt{1 - q_{11}^2}$. Hence, the maximization problem in (43) can be written as:

$$q_1^* = \text{argmax } q_{11}^2 s_{11} + 2q_{11} q_{21} s_{21} + q_{21}^2 s_{22} \quad \text{s.t.} \quad q_1' q_1 = 1. \tag{39}$$

As S is positive semi definite $q_{11}^2 s_{11} \geq 0$ and $q_{21}^2 s_{22} \geq 0$. To achieve the maximum the middle term of the sum has to be positive. As $q_{11} \geq 0$ this term is positive if q_{21} and s_{21} have the same sign. Hence, $q_{21} = \pm\sqrt{1 - q_{11}^2}$ is implicitly normalized to be the same sign as s_{21} due to the maximization in the Max-Share framework.

With the normalization of q_{21} the contribution to the FEV, $\Omega_{1,1}^z(q_{11}) = q_1' S q_1$ has one extreme value at q_{11}^{max} and $\Omega_{1,1}^z(q_{11})$ increases monotonically at $q_{11} \in [0, q_{11}^{max}]$ and decreases monotonically at $q_{11} \in [q_{11}^{max}, 1]$.

Let the true rotation parameter, that yields the true structural parameters, be q_{11}^*. Suppose $q_{11}^* \leq q_{11}^{max}$. According to Condition (a) the inequality restriction $IQ_{i,1,h}(q_{11}) \lesseqgtr \epsilon$ implies a binding linear restriction on q_{11} such that $q_{11} \leq q_{11}^{res}$. Conditions (b) requires that $q_{11}^{res} = q_{11}^*$, and thus the $IQ_{i,1,h}(q_{11})$ implies the inequality constraint $q_{11} \leq q_{11}^*$. As $\Omega_{1,1}^z(q_{11})$ is a strictly increasing function at $q_{11} \in [0, q_{11}^{max}]$

Figure 5: Constraint Maximization of $\Omega_{1,1}(h)$

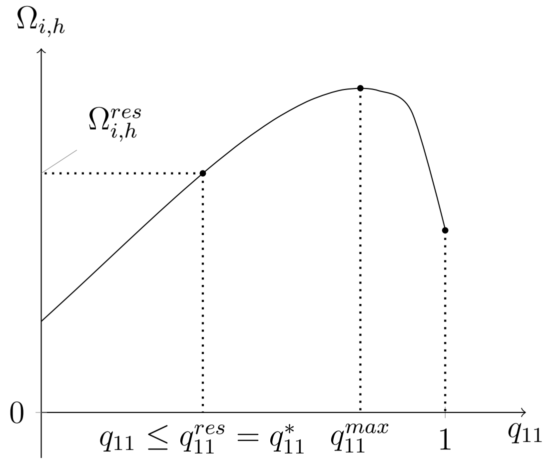

the maximum of the maximization problem (43) augmented with $IQ_{i,1,h}(q_{11}) \lesseqgtr \epsilon$ (which implies $q_{11} \leq q_{11}^{*}$) is at q_{11}^{*}. Figure 5 illustrates the constraint maximization. The very same logic holds when $q_{11}^{max} \geq q_{11}^{*}$ and $IQ_{i,1,h}(q_{11}) \lesseqgtr \epsilon$ implies $q_{11} \geq q_{11}^{res}$.

■

Proof of Proposition 3.4

Let $q_{11} \in [0,1]$ and $IQ_{i,1,h}(q_{11})$ is monotonic at $q_{11} \in [0,1]$. If $IQ_{i,1,h}(q_{11})$ is monotonically increasing it holds that $IQ_{i,1,h}(q_{11}^{low}) \leq IQ_{i,1,h}(q_{11}^{high})$ for all $q_{11}^{low} \leq q_{11}^{high}$.

Figure 6: Linear Constraint on q_{11}

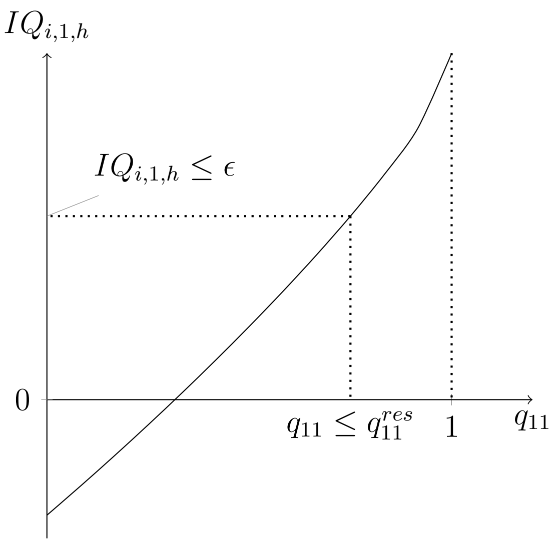

Hence, a linear restriction $IQ_{i,1,h}(q_{11}) \leq \epsilon$ implies a linear restriction $q_{11} \leq q_{11}^{res}$ and $IQ_{i,1,h}(q_{11}) \geq \epsilon$ implies $q_{11} \geq q_{11}^{res}$. Figure 6 illustrates this relationship. The same logic holds true when $IQ_{i,1,h}(q_{11})$ is monotonically decreasing.

■

Checking Condition (a) of Proposition 3.3

More intriguing than the proof of Proposition 3.4 is how to check it for different types of restrictions. The following describes sufficient conditions one can check whether an inequality constraint on $\eta_{i,1,h}$ or $D_{i,h}$ implies a linear constraint on q_{11}.

Firstly, one can check whether $\eta_{i,1,h}(q_{11})$ is monotonic. Let $q_{11} \in [0,1]$. Recall that the impulse response of variable i at horizon h to the first shock is $\eta_{i,1,h} = e_i' C_h B_z q_1$, with e_i being the first column of I_k and

$$C_h B_z = \begin{pmatrix} \Theta_{1,1,h} & \Theta_{1,2,h} \\ \Theta_{2,1,h} & \Theta_{2,2,h} \\ \vdots & \vdots \\ \Theta_{k,1,h} & \Theta_{k,2,h} \end{pmatrix}.$$

Hence, the impulse response function $\eta_{i,1,h}(q_{11})$ is given by:

$$\eta_{i,1,h} = \Theta_{i,1,h} q_{11} + \Theta_{i,2,h} q_{21} = \underbrace{\Theta_{i,1,h} q_{11}}_{\text{A}} + \underbrace{\Theta_{i,2,h} q_{21}}_{\text{B}}. \tag{40}$$

In practice one can carry out the unrestricted Max-Share framework - with fixing q_{11} to be positive - and get q_{11}^{max} and q_{21}^{max} to calculate terms A and B. If the signs of A and B are the opposite $\eta_{i,1,h}(q_{11})$ is monotonic at $q_{11} \in [0,1]$, and thus a linear restriction on $\eta_{i,1,h}(q_{11})$ implies a linear restriction on q_{11}.

For the constraint on the difference in the impulse responses of variable i at horizon h to the two identified shocks $D_{i,h}$ one can also check whether the function $D_{i,h}(q_{11})$ is monotonic. The following describes the steps of Algorithm 3 in the main text.

$$D_{i,h} = \eta_{i,1,h} - \eta_{i,2,h} = e_i' C_h B_z q_1 - e_i' C_h B_z q_2, \tag{41}$$

where e_i is again the first column of I_k. This difference can also be written as:

$$\begin{aligned} D_{i,h} &= (CB_{i,h,1} q_{11} + CB_{i,h,2} q_{21}) - (CB_{i,h,1} q_{12} + CB_{i,h,2} q_{22}) \\ &= CB_{i,h,1}(q_{11} - q_{12}) + CB_{i,h,2}(q_{21} - q_{22}). \end{aligned}$$

Due to the properties of 2×2 orthonormal matrices $q_{22} = \pm q_{11}$ and $q_{12} = \pm q_{21}$. It must hold that if q_{12} and q_{22} have opposite signs, the sings of q_{11} and q_{21} are the same and vice versa. Hence, the relative sign of the entries of the second column q_2 of Q depend on the first column. Yet, whether q_{22} is negative or positive depends on the sign normalization of the second column. Dependent on the sign normalization of q_2 the difference can be written as a function of q_{11}:

$$D_{i,h}(q_{11}) = \underbrace{(CB_{i,h,1} - CB_{i,h,2})}_{\text{A}} q_{11} + \underbrace{(CB_{i,h,1} + CB_{i,h,2})}_{\text{B}} q_{21} \quad \text{if } q_{22} \geq 0 \tag{42}$$

$$D^{-}_{i,h}(q_{11}) = \underbrace{(CB_{i,h,1} + CB_{i,h,2})}_{\text{B}} q_{11} + \underbrace{(CB_{i,h,2} - CB_{i,h,1})}_{\text{-A}} q_{21} \quad \text{if } q_{22} \leq 0, \tag{43}$$

where again $q_{21} = \pm\sqrt{1 - q_{11}^2}$. The sign of q_{21} is determined by the Max-Share maximization, i.e. by q_{21}^{max}. The sign normalization, though, comes from the specification of the constraint. In order for $D_{i,h}$ to truly be a difference $\eta_{i,1,h}$ and $\eta_{i,2,h}$ need to have the same sign. Hence, q_2 is normalized such that $\eta_{i,1,h} = C_h B_z q_1^{max}$ and $\eta_{i,2,h} = C_h B_z q_2$ have the same sign. From the normalization of q_2 one knows whether the difference is written as (42) or (43). If one assesses (42) and q_{21}^{max} is positive, A and B need to have opposite sign in order for $D_{i,h}(q_{11})$ to be monotonic at $q_{11} \in [0, 1]$. If q_{21}^{max} is negative the signs of A and B need to be the same. If one assesses (43) and q_{21}^{max} is positive, A and B need to have same sign in order for $D_{i,h}(q_{11})$ to be monotonic at $q_{11} \in [0, 1]$. If q_{21}^{max} is negative the signs of A and B need to be the opposite.

If the sufficient condition of monotonicity does not hold for the chosen $IQ_{i,1,h}(q_{11})$ one can nevertheless assess whether condition (a) of Proposition 3.3 is satisfied.

Figure 7: Linear Constraint on q_{11} without Monotonicity

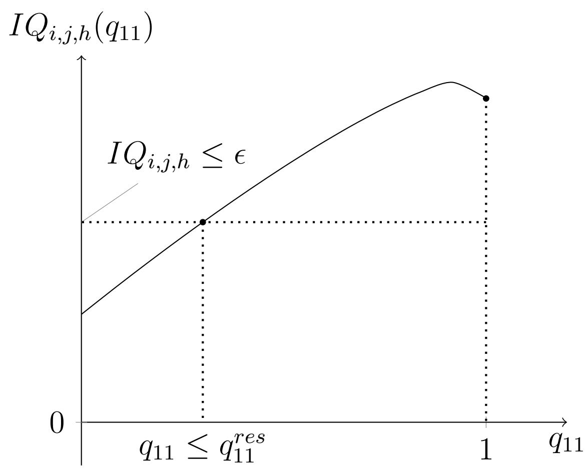

Figure 7 illustrates that $IQ_{i,j,h}(q_{11}) \leq \epsilon$ implies a linear restriction on q_{11} at $q_{11} \in [0, 1]$ if the function value of $IQ_{i,j,h}(q_{11}) = \epsilon$ is unique, i.e. this equality is fulfilled for a single value q_{11}^{res} again at $q_{11} \in [0,1]$. Hence, if $IQ_{i,j,h}(q_{11}) \leq \epsilon$ does not constrain a monotonic function in q_{11} over the relevant domain, checking whether the function value ϵ is unique at $q_{11} \in [0,1]$ allows to establish whether condition (a) of Proposition 3.3 is satisfied nevertheless.

Proof of Proposition 3.5 Let $q_{11} \in [0,1]$. Let $\delta_{i,j,h} = \eta_{i,j,h}(q_{11}^{*}) - \eta_{i,1,h}(q_{11}$ be the bias of the structural impulse response of variable i at horizon h to shock j. Suppose $q_{11}^{max} < q_{11}^{res} < q_{11}^{*}$. If $\eta_{i,j,h}(q_{11})$ is strictly monotonically increasing at $q_{11} \in [q_{11}^{max}, q_{11}^{*}]$, then $\eta_{i,j,h}(q_{11}^{max}) < \eta_{i,j,h}(q_{11}^{res}) < \eta_{i,j,h}(q_{11}^{*})$ and $\delta_{i,j,h}^{res} < \delta_{i,j,h}^{max}$. The same logic holds for $q_{11}^{max} > q_{11}^{res} > q_{11}^{*}$ and/or for strictly decreasing functions. Hence, if q_{11}^{res} approaches q_{11}^{*} from q_{11}^{max}, $|\delta_{i,j,h}|$ decreases. ∎

B Appendix B

Figure 8: 95% Point Estimate Bands, $\epsilon = 0.2$

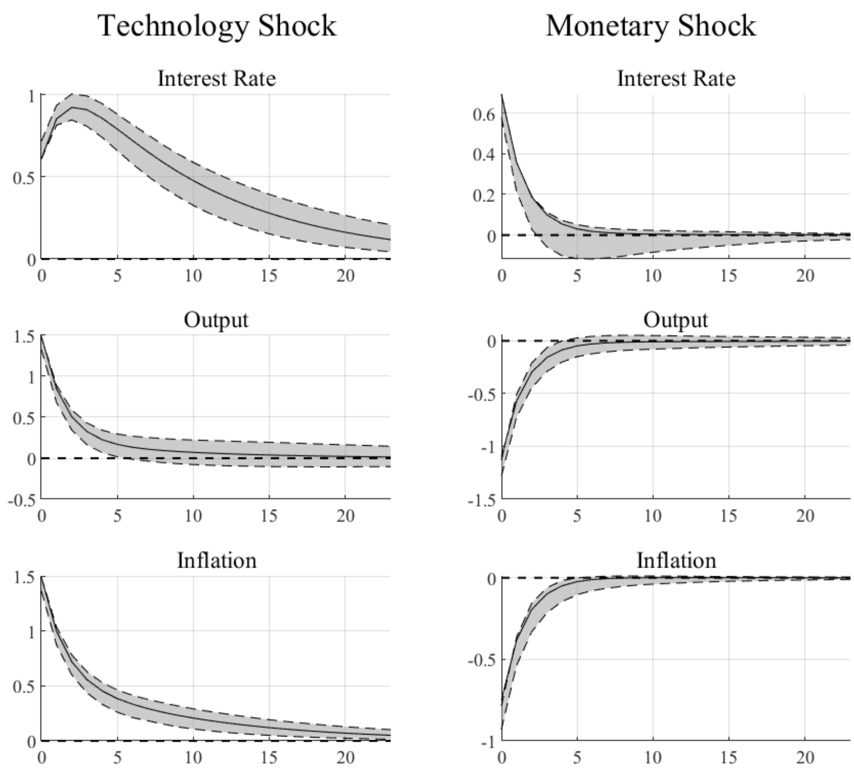

The solid lines are the true impulse responses and the dashed lines are the 2.5% and 97.5% quantile of the solutions found for the 1,000 simulation iterations.

Table 4: Bias of the IRFs to the Technology Shock, $T = 250$ - Scenario B

Variable	$h = 0$	$h = 6$	$h = 12$	$h = 18$
Technology Shock with $\epsilon = 0.38$				
r_t	0.0023	-0.0745	-0.0736	-0.0473
x_t	-0.0084	-0.0381	-0.0173	-0.0059
π_t	-0.0072	-0.0576	-0.0398	-0.0219
Technology Shock with $\epsilon = 0.2$				
r_t	0.0484	-0.0748	-0.0739	-0.0474
x_t	-0.0846	-0.0394	-0.0171	-0.0058
π_t	-0.0607	-0.059	-0.0399	-0.0219
Technology Shock with $\epsilon = 0$				
r_t	0.0956	-0.0795	-0.0764	-0.0485
x_t	-0.1803	-0.0421	-0.0176	-0.006
π_t	-0.1302	-0.0624	-0.0409	-0.0224
Monetary Shock with $\epsilon = 0.38$				
r_t	-0.0026	-0.0105	-0.003	-0.0001
x_t	-0.0016	0.0032	0.0049	0.0039
π_t	-0.005	-0.0046	-0.0003	0.0004
Monetary Shock with $\epsilon = 0.2$				
r_t	-0.0465	-0.0561	-0.0249	-0.011
x_t	-0.1053	-0.0041	0.0017	0.0021
π_t	-0.1082	-0.024	-0.0093	-0.0042
Monetary Shock with $\epsilon = 0$				
r_t	-0.0986	-0.1052	-0.0486	-0.0228
x_t	-0.2086	-0.011	-0.0012	0.0005
π_t	-0.2146	-0.0449	-0.0189	-0.0092

The table depicts the average bias in the estimated structural parameters over the 1,000 Monte-Carlo simulation iterations. The estimates are derived with the Max-Share$^+$ framework in the proxy VAR with different values of ϵ.

Figure 9: Bias of the IRFs to the Technology Shock, $T = 250$ - Scenario B

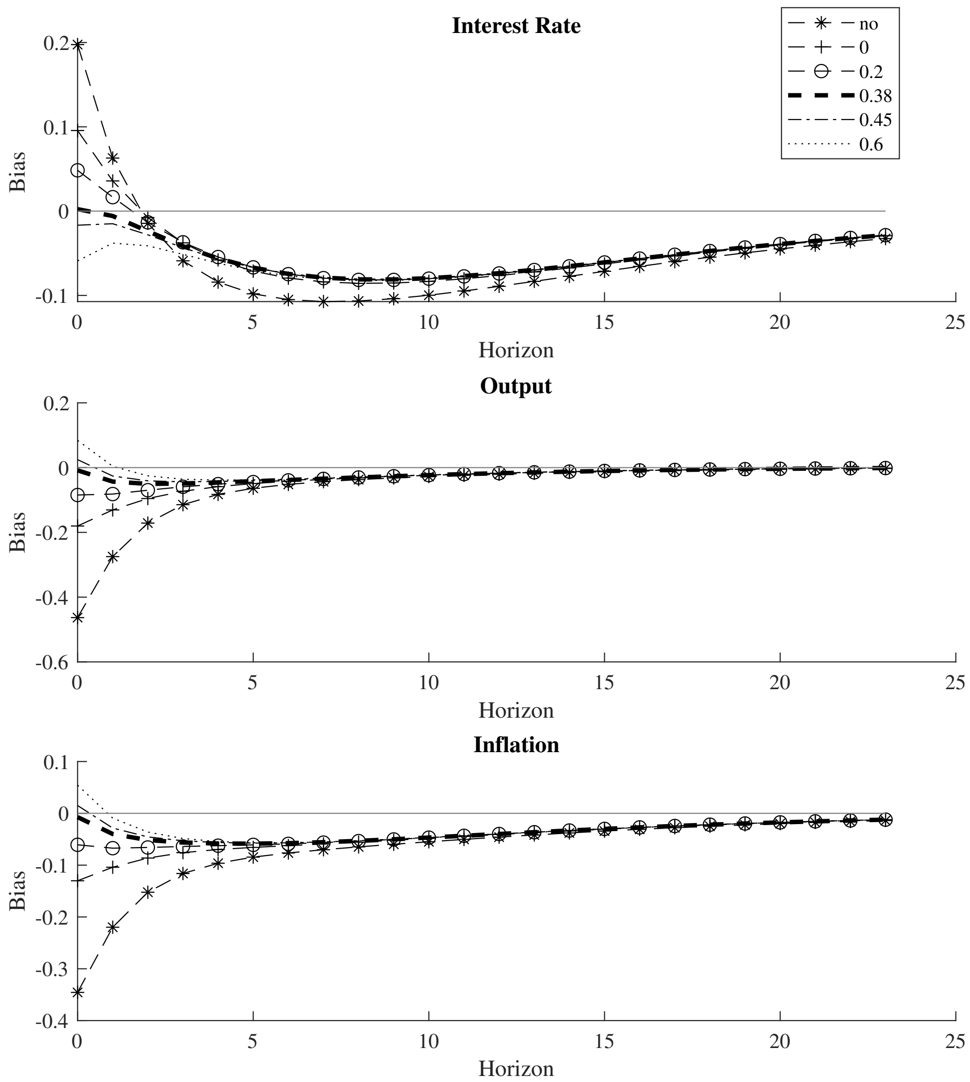

The different lines depict the average bias of the impulse response functions over 1,000 Monte-Carlo simulations for different values of ϵ.

Figure 10: Bias of the IRFs to the Monetary Shock, $T = 250$ - Scenario B

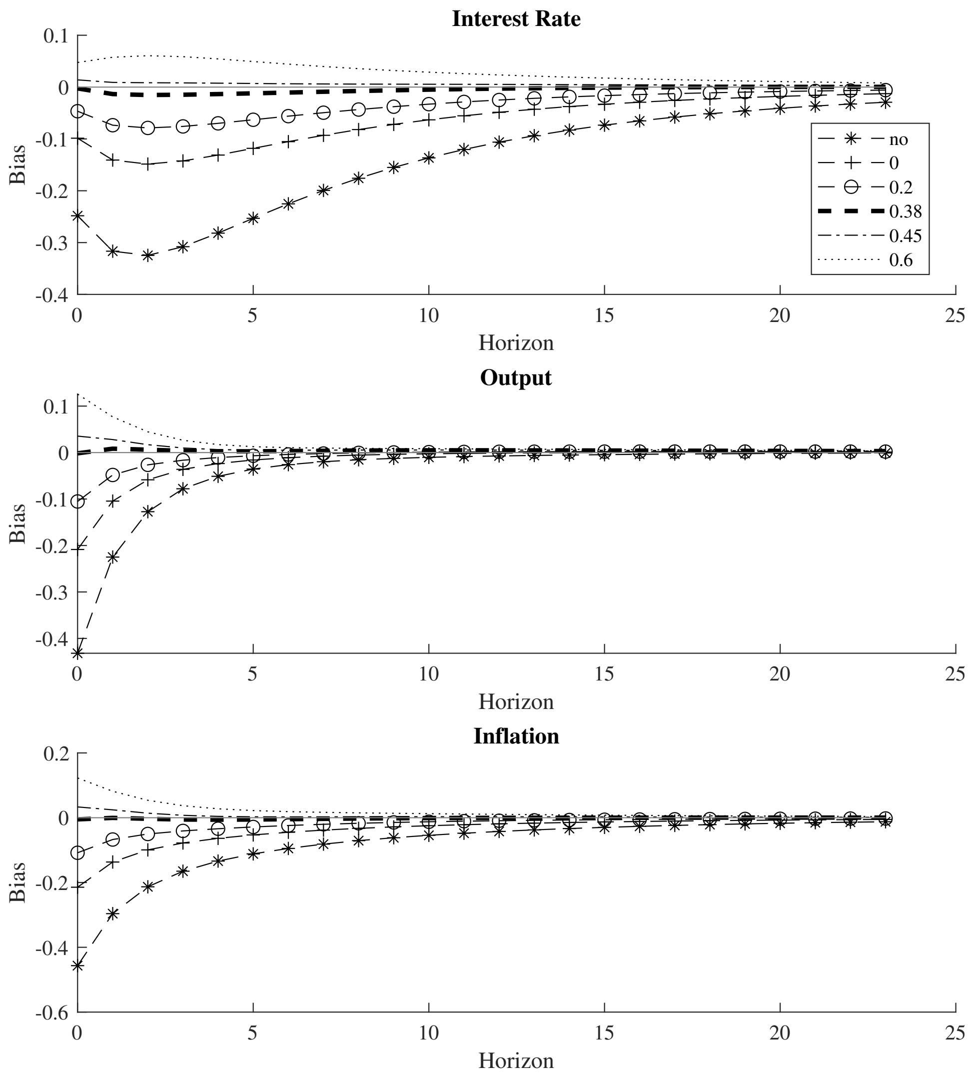

The different lines depict the average bias of the impulse response functions over 1,000 Monte-Carlo simulations for different values of ϵ.

Figure 11: Point Estimate Bands and Sign Restriction Sets, $\epsilon = 0$.

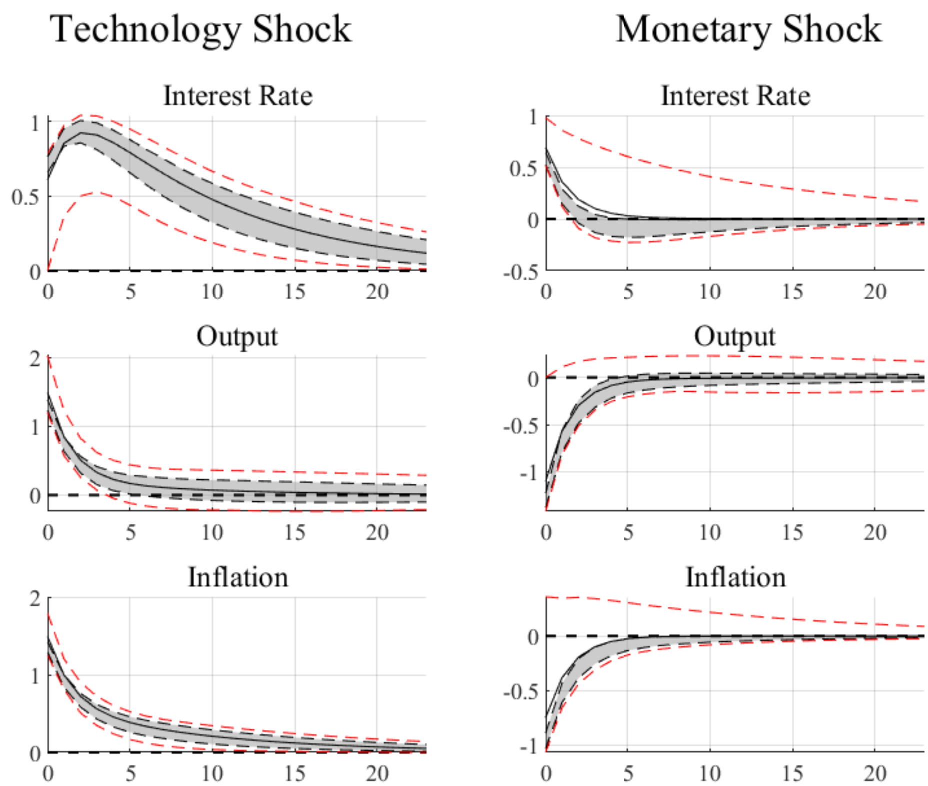

The solid lines are the true impulse responses and the dashed lines are the 2.5% and 97.5% quantile of the solutions found for the 1,000 simulation iterations. The red dashed line are the maximum and minimum responses of the identified set of the proxy SVAR disentangled via pure sign restrictions. The sign restrictions correspond to the constraints of the maximization problem.